

Report 80-3

April 1980

T-28 AIRCRAFT OBSERVATIONS OF THE INTERIOR  
CHARACTERISTICS OF FLORIDA THUNDERSTORMS  
DURING TRIP '78

By: Paul L. Smith, Jr., and Dennis J. Musil

Prepared for:

Meteorology Program  
Division of Atmospheric Sciences  
National Science Foundation  
1800 G Street N.W.  
Washington, DC 20550

Grant No. ATM78-17326

Institute of Atmospheric Sciences  
South Dakota School of Mines and Technology  
Rapid City, South Dakota 57701

## TABLE OF CONTENTS

	<u>Page</u>
1. INTRODUCTION . . . . .	1
2. PARTICIPATION IN THE TRIP 1978 FIELD PROGRAM . . . . .	2
2.1 Description of the T-28 Research Aircraft . . . . .	2
2.2 Summary of T-28 Operations in TRIP '78 . . . . .	5
2.3 Synopsis of Data . . . . .	7
2.4 Data Quality . . . . .	8
3. OBSERVATIONS ON 13 AUGUST 1978 . . . . .	11
3.1 Meteorological Situation . . . . .	11
3.2 Storm Penetrations and Radar Reflectivity Data . . . . .	11
3.3 Hydrometeor Characteristics . . . . .	22
3.3.1 Cloud droplets . . . . .	22
3.3.2 Ice particles observed by the PMS 2D probe . . . . .	22
3.3.3 Precipitation particles . . . . .	26
3.4 Updraft and Thermodynamic Data . . . . .	30
3.5 Disposition of Condensed Water in the Clouds . . . . .	36
4. OBSERVATIONS ON OTHER RESEARCH DAYS . . . . .	39
4.1 Data from 9 August 1978 . . . . .	39
4.2 Data from 10 August 1978 . . . . .	41
4.3 Data from 12 August 1978 . . . . .	42
5. SUMMARY AND CONCLUSIONS . . . . .	48
5.1 Summary of Significant Observations . . . . .	48
5.2 Inferences Regarding Precipitation Processes . . . . .	49
5.3 Inferences Regarding Electrification Processes . . . . .	50
ACKNOWLEDGMENTS . . . . .	53
REFERENCES . . . . .	54

## LIST OF FIGURES

<u>Number</u>	<u>Title</u>	<u>Page</u>
1	View of armored T-28 aircraft in flight . . . . .	3
2	KSC sounding for 0905 GMT, 13 Aug 1978 . . . . .	12
3	T-28 track for Penetration 1 on 13 Aug 1978 superimposed on contoured slant range radar PPI presentation . . . . .	14
4	Same as Fig. 3 except for Penetration 2 . . . . .	15
5	Same as Fig. 3 except for Penetration 3 . . . . .	16
6	Same as Fig. 3 except for Penetration 4 . . . . .	17
7	Same as Fig. 3 except for Penetration 5 . . . . .	18
8	Same as Fig. 3 except for Penetration 6 . . . . .	19
9	Same as Fig. 3 except for Penetration 7 . . . . .	20
10	Same as Fig. 3 except for Penetration 8 . . . . .	21
11	A cloud droplet spectrum from an updraft region encountered during Penetration 7 on 13 Aug 1978 . . . . .	23
12	Comparison of cloud liquid water concentrations measured by the PMS FSSP and the J-W sensor during Penetration 7 on 13 Aug 1978 . . . . .	24
13	Sample of PMS 2D probe particle image data from an updraft region of Penetration 7 on 13 Aug 1978 . . . . .	25
14	Example of dendritic or aggregate particles observed by the PMS 2D probe during Penetration 8 on 13 Aug 1978 . . . . .	27
15	Particle camera frame from Penetration 2 on 13 Aug 1978 . . . . .	28
16	Particle camera frame from Penetration 1 on 13 Aug 1978 . . . . .	29
17	Plot of measured and computed variables vs. time for most of Penetration 1 on 13 Aug 1978 . . . . .	31

## LIST OF FIGURES (continued)

<u>Number</u>	<u>Title</u>	<u>Page</u>
18	As Fig. 17 but for portion of Penetration 2 on 13 Aug 1978 containing significant updrafts . . . . .	32
19	As Fig. 17 but for Penetration 3 on 13 Aug 1978 . . . . .	33
20	As Fig. 17 but for Penetration 6 on 13 Aug 1978 . . . . .	34
21	As Fig. 17 but for Penetration 7 on 13 Aug 1978 . . . . .	35
22	Particle camera frame from Penetration 6 on 13 Aug 1978 . . . . .	36
23	Sample of PMS 2D probe particle image data from the updraft region of Penetration 5 on 10 Aug 1978 . . . . .	43
24	Example of larger graupel and dendritic or aggregate particles observed by the PMS 2D probe during Penetration 2 on 10 Aug 1978 . . . . .	44
25	Sample of PMS 2D probe data from Penetration 9 on 10 Aug 1978 showing 2 spherical particles joined together . . . . .	45
26	Sample of PMS 2D probe data from Penetration 18 on 12 Aug 1978 showing graupel and columns observed in a weak thunderstorm updraft . . . . .	46
27	Example of aggregate-type particles observed by the PMS 2D probe during Penetration 5 on 12 Aug 1978 . . . . .	47
28	Results of cloud liquid water depletion calculations for a portion of Penetration 7 on 13 Aug 1978 . . . . .	51

## LIST OF TABLES

<u>Number</u>	<u>Title</u>	<u>Page</u>
1	T-28 Instrumentation Complement . . . . .	3
2	Summary of T-28 TRIP Flight Operations (1 - 17 August 1978) . . . . .	6
3	Summary Data for TRIP '78 Cloud Penetrations . . .	9
4	Comparison of Hydrometeor Mass Concentrations Observed on 13 Aug 1978 with Adiabatic Values . . .	37

## 1. INTRODUCTION

This is the final report on research carried out as part of the 1978 Thunderstorm Research International Program (TRIP '78) with support under National Science Foundation (NSF) Grant No. ATM 78-17326. The TRIP is a cooperative effort among several participating groups of scientists interested in studying the electrical processes and properties of thunderstorms (Pierce, 1976). The program includes a variety of experiments aimed at determining the characteristics of electric fields and lightning discharges in thunderstorms and the locations and magnitudes of charge centers aloft (see, e.g., Livingston and Krider, 1978). It also includes Doppler and rapid-scan radar studies of the storms (e.g., Lhermitte, 1978) and investigations of precipitation particle size distributions and particle charges (e.g., Gaskell *et al.*, 1978). Field investigations under TRIP were carried out at the Kennedy Space Center (KSC), Florida, from the summers of 1976 through 1978.

The Institute of Atmospheric Sciences (IAS) participated briefly in the 1978 field program to obtain in situ observations from the storm interiors with its T-28 research aircraft. This participation was a cooperative effort involving the Convective Storms Division (CSD) of the National Center for Atmospheric Research (NCAR) along with the IAS. The aircraft is specially armored for penetrating thunderstorms that may contain hail and is equipped with an elaborate meteorological instrumentation system. The main purpose of the participation in TRIP was to obtain information about the updraft structures and hydrometeor characteristics of the Florida thunderstorms. Such information is useful to other scientists participating in TRIP in interpreting their own observations of other storm characteristics and in understanding cloud electrification processes. The IAS and CSD also undertook a modest analysis effort to evaluate some of the more interesting data in terms of their implications regarding precipitation processes in the storms.

## 2. PARTICIPATION IN THE TRIP 1978 FIELD PROGRAM

### 2.1 Description of the T-28 Research Aircraft

The T-28 is a low-wing monoplane with a radial engine (Fig. 1). The South Dakota School of Mines and Technology (SDSMT) T-28 system was developed for the purpose of studying the interior characteristics of thunderstorms and hailstorms. Critical wing and tail surfaces of the plane are armored and the cockpit canopy and engine housing strengthened to permit penetrations through storms containing hail up to about 7.6 cm (3 inches) in diameter. The aircraft was used in thunderstorm research projects in the northern Great Plains (Colorado and South Dakota) from 1969 through 1978, accumulating over 300 storm penetrations.

The aircraft is equipped with a unique complement of meteorological instruments emphasizing observations of cloud microphysics. The instrumentation carried on the T-28 during 1978 is summarized in Table 1 (see also Johnson *et al.*, 1978). Many of the instruments belong to the NCAR-CSD but are made available for research such as the TRIP investigations under a cooperative agreement between SDSMT and NCAR.

Altitude values and rate-of-climb data for updraft calculations are derived from the static pressure measurements. In-cloud temperature values are obtained from the NCAR reverse flow probe, which is much less subject to wetting than the Rosemount instrument. The hydrometeor sensors cover the entire size range from cloud droplets through hailstones, as follows (values of the approximate sampling volume per unit time are given in parentheses for each instrument):

- a. Cloud droplets (up to 30-50  $\mu\text{m}$  in diameter): Johnson-Williams cloud liquid water concentration sensor ( $0.05 \text{ m}^3 \text{ s}^{-1}$ ); Particle Measuring Systems FSSP probe ( $3.7 \times 10^{-5} \text{ m}^3 \text{ s}^{-1}$ ).
- b. Intermediate (embryo) size range (30-1000  $\mu\text{m}$  in diameter): Particle Measuring Systems two-dimensional optical array probe ( $0.01 \text{ m}^3 \text{ s}^{-1}$ ); Cannon particle camera (up to  $0.6 \text{ m}^3 \text{ s}^{-1}$ ).
- c. Raindrops and graupel (submillimeter up to about 1 cm in diameter): Continuous hydrometeor sampler (foil impactor;  $0.15 \text{ m}^3 \text{ s}^{-1}$ ); Cannon particle camera.
- d. Hailstones (4 mm to over 5 cm in diameter): Hail spectrometer ( $10 \text{ m}^3 \text{ s}^{-1}$ ); foil impactor.

The hail spectrometer and the particle camera cannot be carried simultaneously on the T-28 because of space, weight, and electrical power limitations. The hail spectrometer was designed to determine



Fig. 2: View of armored T-28 aircraft in flight. Cannon camera device consisting of white pod housing film transport, rotating mirror and control electronics, and black flash system is shown on the aircraft's left wing. The reverse flow temperature device (with exhaust ports) is outboard from the Cannon camera. The FSSP and 2-D Particle Measuring Systems probes are shown on the pylon of the right wing, with the foil impactor located between the probes. Outboard from these instruments are the angle-of-attack and the Johnson-Williams Liquid Water devices. [Photo by Roger Rozelle - AOPA Pilot Magazine]



TABLE 1  
T-28 Instrumentation Complement

<u>Variable</u>	<u>Instrument</u>	<u>Range of Measurement</u>
<u>State:</u>		
Static Pressure (Altitude)	Rosemount 1301-A-4-B Ball Engineering EX-210-B	0 to 15 PSI 0 to 27,000 ft (8.2 km) MSL
Total Temperature	Rosemount 102AU2AP, platinum wire NCAR Reverse Flow, diode	-25 to +25°C -25 to +25°C
<u>Hydrometeors:</u>		
Cloud droplets	Johnson-Williams LWC Particle Measuring Systems FSSP	<50 $\mu\text{m}$ dia (liquid only); 0 to 6 $\text{g m}^{-3}$ 3 to 45 $\mu\text{m}$ dia; adjustable
Rain, graupel, snow	Williamson Foil Impactor Particle Measuring Systems OAP-2D Cannon Particle Camera (alternates with hail spectrometer)	1 to 20 mm dia 31 to 1000 $\mu\text{m}$ Approx. 50 $\mu\text{m}$ up
Hail	IAS Laser Hail Spectrometer (alternates with Cannon camera)	4.5 to 50+ mm dia
<u>Aircraft Navigation &amp; Performance:</u>		
Attitude	Servomechanisms TR541 angle-of-attack vane Pitch (Humphrey vertically-stabilized accelerometer) Roll (Humphrey vertically-stabilized accelerometer)	-15 to +15° -50 to +50° -50 to +50°
Navigation	IAS Heading indicator NARCO UDI-2ARD DME CESSNA 400 DME NARCO MK12 VOR (2 units) NARCO NAV-122 VOR	0 to 360° magnetic 0 to 100 n mi 0 to 100 n mi 0 to 360° from 0 to 360° from
Performance	Ball Engineering 101A variometer (rate-of-climb) Rosemount 1301-D-1-B dynamic pressure (ind. airspeed) NCAR True Airspeed Computer Humphrey SA09-D0101-1 vertically- stabilized accelerometer Giannini 45218YE manifold pressure	-6000 to +6000 $\text{ft min}^{-1}$ (-30 to +30 $\text{m s}^{-1}$ ) -3 to +3 PSI 0 to 250 knots (128 $\text{m s}^{-1}$ ) -1 to +3 g's 0 to 50+ in Hg

the sizes and concentrations of particles larger than about 4 mm in diameter. Few such particles were expected in the Florida storms, and because the T-28 operating period in TRIP '78 was brief, only the particle camera was used in Florida. That instrument provides an effective way of distinguishing between liquid and ice particles. On the film, water drops are indicated by pairs of dots with spacings approximately equal to the drop diameters. Ice particles appear as full back-lighted images.

The primary data recording system on the T-28 records the outputs of most of the instruments listed in Table 1, along with time, on 7-track, computer-compatible, magnetic tape. The basic recording interval is once per second, but some variables are sampled twice during each one-second cycle to provide higher frequency response. A second digital magnetic tape deck records the particle data from the PMS probes and also serves as a backup recorder for other key variables. An audio recorder serves as a "notebook" to record the pilot's in-flight comments. A second channel records the sounds of hail impacts on the windscreen, which are helpful in correlating the other observations of hailstones.

## 2.2 Summary of T-28 Operations in TRIP '78

The T-28 was flown from Laramie, Wyoming, to Florida after completion of the 1978 NCAR-CSD field program in northeast Colorado. It arrived at Patrick Air Force Base on 2 August 1978, while the rest of the regular field personnel arrived with the ground support equipment on 4 August.

The field team included the project meteorologist, pilot, research engineer, and aircraft mechanic/technician from the IAS, and an electronics technician from the NCAR-CSD. The T-28 was hangared in the NASA Flight Operations Facility at Patrick AFB, and all personnel except the meteorologist were based at Patrick. The meteorologist was stationed in the TRIP weather operations room at KSC about 20 miles north of Patrick, from where he directed the T-28 storm penetrations.

By the time the T-28 arrived in Florida, operations of the other aircraft that participated in TRIP '78 (a NASA Beech D-18, an Air Force T-39, and a Naval Research Laboratory S-2D) had been completed. Thus the TRIP '78 T-28 investigations were not conducted as part of a coordinated flight program. However, most of the TRIP ground-based experiments were still operational during the T-28 research flights, and coordination was effected with those experiments.

The main role of the T-28 was to collect in-storm observations that could be reduced and organized in a way useful in complementing the extensive set of electric field, lightning, radar, and other observations collected. The T-28 TRIP '78 flight operations are summarized in Table 2. A communications and tracking check flight was made on

TABLE 2

Summary of T-28 TRIP Flight Operations  
1 - 17 August 1978

Date (1978)	Flight No.	Time (hrs)	Approximate Research Time Block (EDT)	Penetrations	Data Recorded*				Remarks	
					PI Tape	Pertec Tape	Voice Tape	Voice Tape		
8/1	239	2.6							Ferry to Wichita, KS	
8/1	240	2.6							Ferry to Memphis, TN	
8/1	241	1.9							Ferry to Atlanta, GA	
8/2	242	3.0							Ferry to Patrick AFB, FL	
8/8	243	1.6							Communications and tracking check	
8/9	244	2.1	1523-1616	9	Yes	No	Yes	Yes	Research	
8/10	245	1.5	1205-1237	10	Yes	Yes	Yes	Yes	Research	
8/10	246	0.8			Yes	Yes	Yes	Yes	Research - clouds dissipated	
8/12	247	2.3	1122-1224	18	Yes	Yes	Yes	Yes	Research	
8/13	248	1.7	1516-1605	8	Yes	Yes	Yes	Yes	Research	
8/15	249	2.5							Ferry to Atlanta, GA	
8/16	250	2.4							Ferry to Greenville, MS	
8/16	251	2.2							Ferry to Dallas, TX	
8/17	252	2.0							Ferry to Wichita, KS	
8/17	253	2.7							Ferry to Cheyenne, WY	
8/17	254	1.4							Ferry to Rapid City, SD	
<u>Totals</u>										
Total number of flights				16	Total aircraft flight hours				33.3	
Total number of research flights				5	Total number of cloud penetrations				45	

\*Cannon particle camera carried on all flights. PI Tape: Basic aircraft instrumentation data.  
Pertec Tape: PMS probe data. Voice Tape: Pilot comments plus hailstone impacts on windscreens.

8 August. There were four subsequent research flights resulting in 45 cloud penetrations, plus a fifth research flight which produced no data because of extremely rapid cloud dissipation following takeoff. One intended quick-turn-around research flight on 12 August had to be cancelled because of electrical activity in the vicinity of Patrick AFB. It is Air Force policy not to refuel aircraft when an electrical storm is within five miles, as was the case on that day. The T-28 departed Patrick AFB on 15 August after research opportunities had been exhausted.

No major difficulties were encountered with either the aircraft or the instrumentation. One unforeseen problem came up because of the limited defogging system in the T-28. After the airplane had been at altitude for some time during a research flight, descent to the warm and humid lower levels (below about 4000 ft altitude) resulted in heavy condensation, beyond the defogging capability, inside the canopy and windscreen. With no outside visibility, about 15 minutes of circling at lower altitudes was necessary until the aircraft warmed sufficiently to evaporate the condensation and make a landing possible. The result was that about 15 minutes less on-station time than normal was available for the research flights.

### 2.3 Synopsis of Data

Research flights were made on four days: 9, 10, 12, and 13 August 1978. The storms of 13 August were selected for primary attention as case studies by the TRIP '78 participants.

Table 3 presents some of the pertinent information for each cloud penetration in Florida. Eight or more penetrations were made on each research flight, but more than one cloud or storm was studied on every flight. The penetration altitudes varied from 5.0 to 7.0 km MSL, and the measured in-cloud temperatures ranged from  $-3^{\circ}\text{C}$  to  $-17^{\circ}\text{C}$ .

Most of the Florida clouds studied were rather small and of short duration. Many of the penetrations were therefore quite short; more than half were less than 9 km in extent. Only small towering cumulus clouds occurred on 10 August, and the longest penetration was 7.5 km. Most of the penetrations on 12 August were also through small towering cumulus, and the length of one penetration on that day was only 1.4 km. The clouds on 12 August developed into weak thunderstorms towards the end of the flight. Larger, mature thunderstorms were studied on both 9 and 13 August, and on the latter date, one penetration was 36 km long.

On 9 and 10 August, the penetrations were made at altitudes below 6 km, with average temperatures mostly from  $-7^{\circ}\text{C}$  to  $-9^{\circ}\text{C}$ . On 12 and 13 August, the penetrations were made at higher altitudes, above 6 km, where the average temperatures ranged from  $-11^{\circ}\text{C}$  to  $-15^{\circ}\text{C}$ . The data from the first "thunderstorm day" (9 August) thus came from relatively warm parts of the supercooled cloud region, around  $-7^{\circ}\text{C}$ , while those

for the second "thunderstorm day" (13 August) came from somewhat colder regions of the storms, around  $-13^{\circ}\text{C}$ . Comparison of observations from those two days leads to some interesting inferences about the precipitation mechanisms in the Florida storms, as discussed in Section 5.

The peak updraft speed exceeded  $20\text{ m s}^{-1}$  on three occasions during thunderstorm penetrations, once each on 9, 12, and 13 August. However, the median peak updraft observed during the 45 penetrations was only  $6\text{ m s}^{-1}$ . The strongest observed downdraft was about  $12\text{ m s}^{-1}$ , while typical downdraft speeds were 6 to  $8\text{ m s}^{-1}$ .

Table 3 shows that the cloud liquid water concentrations measured by the Johnson-Williams (J-W) sensor were small, being essentially always less than  $0.5\text{ g m}^{-3}$ . The single exception was an observed maximum of  $0.6\text{ g m}^{-3}$  on Penetration No. 6 on 9 August; the updraft during that penetration was 5 degrees more buoyant than the air surrounding the cloud. There are some indications that the J-W liquid water sensor on the T-28 may indicate values that are somewhat low; this problem would be accentuated by the presence of large cloud droplets in maritime clouds like those encountered in Florida. Even after allowing for those factors, the observed cloud liquid water concentrations were very small compared to the potential values computed for adiabatic parcel ascent to the altitudes at which the T-28 was flying. The minimal airframe icing during the penetrations also suggests that the cloud liquid water concentrations were low. These observations of low amounts of cloud liquid water suggest certain inferences about the precipitation mechanism that are discussed in Section 3.3 and later.

#### 2.4 Data Quality

The aircraft data quality was generally good. The pressure (altitude), temperature, updraft, and J-W liquid water concentration data were summarized in Section 2.3. Usable data were obtained from the two PMS probes (FSSP and OAP-2D) on 10, 12, and 13 August, but no PMS data tape was obtained on 9 August. All of the PMS probe data were processed through the sequence of programs described by Heymsfield and Parrish (1979). Artifacts often called "streakers" were prevalent in the 2D probe image data. The "streakers" are thought to be caused by the accumulation, then shedding, of liquid water at the probe tips. This explanation is somewhat at odds with the low observed cloud liquid water concentrations, but cloud droplets too large to be sensed by the J-W instrument could contribute to the shedding problem. There was also some difficulty with the PMS 2D data related to some malfunction in the recording or timing circuitry that caused some of the particle images to be broken up and unrecognizable. These problems made it difficult to analyze important portions of the 2D probe data.

TABLE 3  
Summary Data for TRIP '78 Cloud Penetrations

Date [1978]	Penetration No.	Times [EDT]		Pen. Dist. [km]	Avg. Alt. [km MSL]	Avg. Temp. [°C]	Max. Updraft [m s <sup>-1</sup> ]	Min. Downdraft [m s <sup>-1</sup> ]	Max. J-W LWC [g m <sup>-3</sup> ]
		Entry	Exit						
9 Aug (Flt 244)	1	152302	152745	28.3	5.2	-7	9	-8	0.4
	2	152842	153209	20.7	5.2	-7	11	-8	0.4
	3	153431	153732	18.1	5.2	-7	9	-5	0.2
	4	153932	154130	11.8	5.3	-8	15	-7	0.4
	5	154245	154504	13.9	5.3	-7	4	-7	0.1
	6	154753	155009	13.6	5.5	-6	21	-8	0.6
	7	160741	160956	13.5	5.2	-7	5	-6	0.1
	8	161139	161316	9.7	5.2	-7	7	-5	<0.1
	9	161451	161606	7.5	5.2	-7	5	-10	<0.1
10 Aug (Flt 245)	1	120549	120635	4.6	5.6	-9	4	-4	0.2
	2	120948	121017	2.9	5.5	-8	2	-6	0.2
	3	121324	121408	4.4	5.4	-7	5	-6	<0.1
	4	121700	121720	2.0	5.5	-8	4	-10	0.2
	5	122130	122221	5.1	5.6	-9	4	-6	<0.1
	6	122335	122445	7.0	5.6	-9	3	-8	0.3
	7	122610	122726	7.5	5.5	-8	6	-7	0.2
	8	122908	123016	6.8	5.5	-8	12	-11	0.3
	9	123250	123402	7.2	5.5	-9	6	-8	0.1
	10	123515	123627	7.2	5.6	-9	7	-5	0.2
12 Aug (Flt 247)	1	112301	112427	8.6	6.2	-12	13	-5	0.3
	2	112740	112903	8.3	6.4	-13	10	-5	0.2
	3	113321	113514	11.3	6.5	-13	11	-5	0.1
	4	113828	113945	7.7	6.5	-14	3	-6	0.1
	5	114355	114505	7.0	6.5	-13	4	-6	<0.1
	6	114850	114945	5.5	6.5	-13	2	-5	<0.1
	7	114950	115026	3.6	6.6	-14	11	-4	0.2
	8	115240	115350	7.0	6.5	-13	4	-6	0.1
	9	115600	115631	3.1	6.5	-13	5	-4	0.2
	10	115804	115857	5.3	6.4	-13	4	-10	0.1
	11	120055	120156	6.1	6.5	-13	14	-11	0.1
	12	120316	120517	12.1	6.5	-13	4	-9	0.2
	13	120531	120658	8.7	6.5	-13	9	-9	0.1
	14	120810	120824	1.4	6.4	-13	2	-3	0
	15	120953	121347	23.4	6.5	-13	15	-7	0.2
	16	121550	121741	11.1	6.7	-14	12	-8	0.1
	17	121835	121941	6.6	6.8	-15	23	-8	0.2
	18	122112	122310	11.8	6.8	-15	17	-8	0.1
13 Aug (Flt 248)	1	151645	152041	23.6	6.3	-11	10	-8	0.2
	2	152615	153216	36.1	6.5	-12	16	-9	0.2
	3	153639	153900	14.1	6.6	-13	6	-10	0.2
	4	154232	154600	20.8	6.6	-13	5	-9	<0.1
	5	154950	155309	19.9	6.2	-11	4	-8	<0.1
	6	155344	155602	13.8	6.5	-12	14	-12	0.3
	7	155905	160155	17.0	6.6	-13	22	-11	0.4
	8	160239	160429	11.0	6.8	-15	4	-6	0.1

Foil impactor data were obtained for each research day, and the particle camera film for all the research flights was of excellent quality. Most of the foil and film data have been examined at least roughly, but detailed data reduction was carried out only for selected portions.

There was a C-band tracking radar at KSC and a tracking transponder was installed in the T-28. However, due to an unfortunate set of circumstances involving rocket launchings and KSC staff workloads, no radar tracks of the aircraft were obtained during the research flights. This forced us to rely for position data on the DME/VOR data recorded on board the aircraft, which for the Florida operations were not consistently of the best quality. They were adequate to estimate the T-28 penetration tracks, but the accuracy of the aircraft positions determined from the DME/VOR data is probably no better than 1-2 km.

No quantitative weather radar data were directly available at KSC to aid the project meteorologist in directing the T-28 penetrations. An X-band weather radar with a non-quantitative display was available, and some maximum reflectivity data were relayed by voice from a remote C-band weather radar. In spite of these limitations, a scheme was worked out among the project meteorologist, T-28 pilot, and personnel manning the remote radar so that the penetrations could be made adequately and safely. This arrangement could not produce the desired precision of the penetrations, but good quality data were nevertheless gathered during each research flight. Reflectivity data recorded by the NCAR CP-4 radar system were obtained later so that the locations of the T-28 penetrations could be related to the overall storm structures.

### 3. OBSERVATIONS ON 13 AUGUST 1978

As mentioned previously, the storms that were observed on 13 August were selected for case study analysis by the TRIP participants. Consequently, most of the discussion in this report deals with the T-28 observations from that day. These data are reviewed in this section. Some of the data collected on the other days are discussed in Section 4, mostly as they pertain to comparisons with the observations on 13 August and possible implications regarding the precipitation mechanisms.

#### 3.1 Meteorological Situation

The weather events on 13 August appear to be fairly typical for areas near the east coast of Florida. Small rain showers developed during the late morning along the coast and gradually moved inland while increasing in intensity. The T-28 penetrations were made in mature thunderstorms that occurred in mid-afternoon. A detailed description of the weather for that day has been assembled by personnel manning the weather station at KSC.<sup>1</sup>

Unfortunately only one radiosonde was released from KSC on 13 August due to a misunderstanding between TRIP personnel and the Air Force people conducting the soundings. The sonde was released at 0905 GMT and the sounding (Fig. 2) exhibits a convective condensation level near 0.6 km MSL. The 0°C isotherm was at about 4.4 km MSL, giving a warm cloud depth of about 3.8 km. The low level moisture was 18 g kg<sup>-1</sup> and the sounding was quite unstable, with a lifted index near -7.5. Winds were weak at all levels. Below 350 mb, they were from the southwest at speeds up to 20 kt, while above that they were from the northeast up to 20 kt. Even though this is the only sounding available for this day, it is felt to be representative of the conditions in which the storms developed.

#### 3.2 Storm Penetrations and Radar Reflectivity Data

The T-28 made eight penetrations on 13 August, between approximately 1515 and 1605 EDT. Two different storms were penetrated, and the last penetration was in the decaying portion of a third. Summary data for the penetrations were given previously in Table 3.

The X-band weather radar data available to the project meteorologist for use in directing the T-28 penetrations were not recorded for post-analysis. Therefore, C-band reflectivity data recorded from the NCAR CP-4 Doppler radar located at the TICO airport were analyzed to locate the T-28 penetrations with respect to the storm reflectivity patterns.

---

<sup>1</sup>For information concerning these descriptions, contact Mr. Angelo Taiani, TRIP Project Coordinator at KSC.



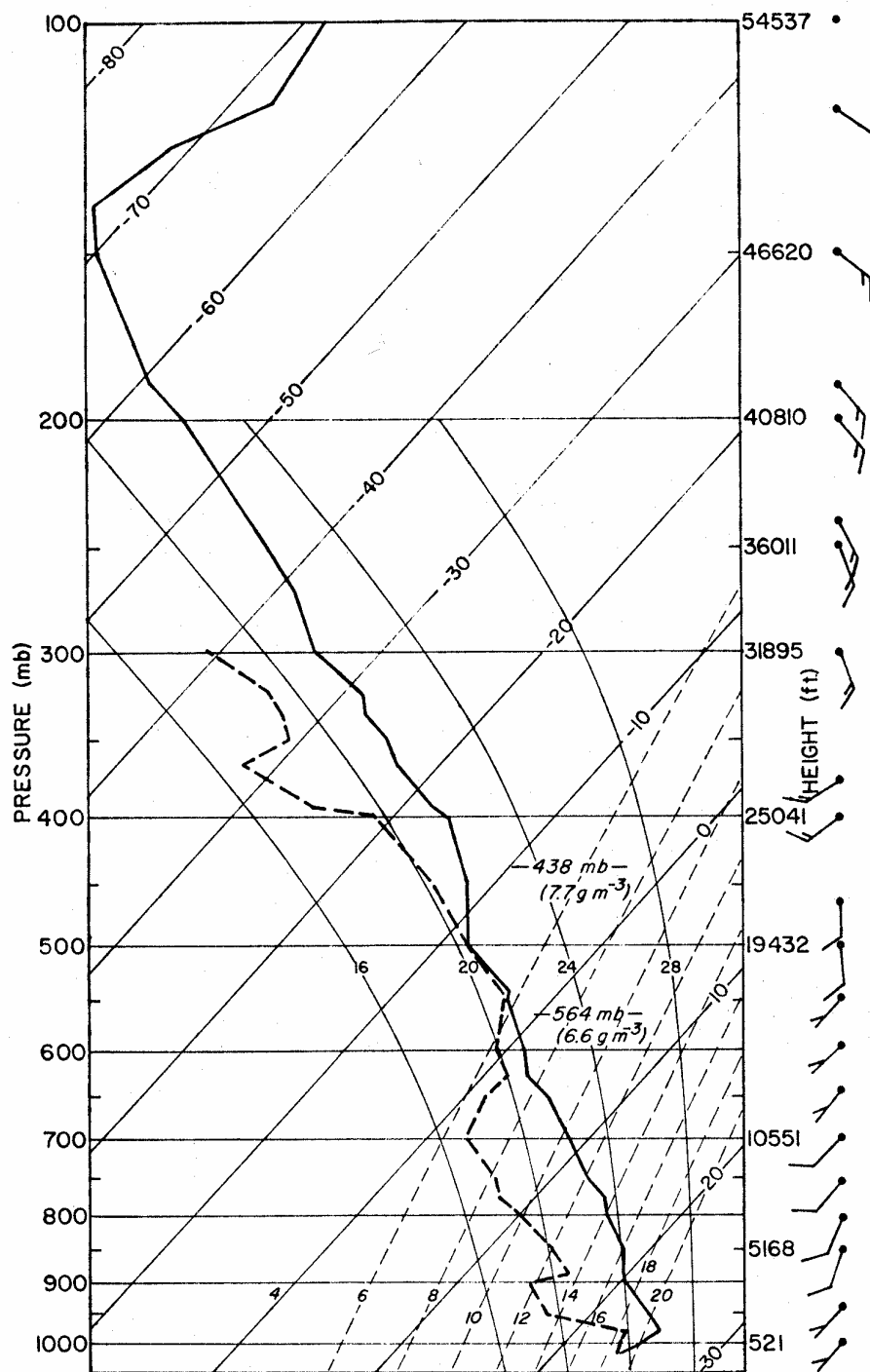


Fig. 2: KSC sounding for 0905 GMT, 13 Aug 1978. Adiabatic condensate concentrations are indicated for 438 and 564 mb levels.

Slant-range PPI patterns near the altitude of the T-28 for each penetration are shown with the penetration tracks superimposed in Figs. 3-10.

The first three penetrations were quite close to, and one even passed over, the radar site. That makes it difficult to obtain radar data applicable to the aircraft locations. The later penetrations were more than 10 km from the radar so that more reasonable representations of the reflectivity structures penetrated by the aircraft can be given. The reflectivity patterns selected were near the times of the T-28 penetrations; however, during Penetration 6, the radar was scanning at high elevations and was looking over the top of the storm being penetrated. Hence the nearest radar data were about 7 min away.

The radar data show strong storm development almost directly over the radar site. The data may be contaminated by the presence of ground clutter echoes that could not be separated out. This also makes analysis of the radar data difficult, especially for the first three penetrations. The storms began to develop further from the radar later during the flight and the ground clutter problem diminished greatly, especially for the last three penetrations.

Penetrations 1 through 3 went through a storm directly over the TICO Airport, while Penetrations 4 and 5 went through the northern edge of that same storm. Penetrations 6 and 7 were made through a different storm 20 to 30 km northwest of the radar, while No. 8 passed through what appears to be the decaying portion of still another storm.

Penetration No. 7 is of particular interest because the last part of the penetration apparently went through a maximum reflectivity area of about 55 dBz. This penetration also yielded the strongest updraft ( $22 \text{ m s}^{-1}$ ) and the highest cloud liquid water concentration ( $0.4 \text{ g m}^{-3}$ ) observed on 13 August. Two updraft areas were found, centered about 6 km apart and each about 3 km wide. The first, with maximum updraft speed around  $18 \text{ m s}^{-1}$ , was just southwest of the maximum reflectivity region (Fig. 9). The second, stronger one was near the northeast edge of the cell. The indicated track for that penetration is quite consistent with the hydrometeor observations made by the T-28. It is fortuitous that such a penetration occurred, because the only real-time quantitative radar reflectivity measurements available to assist the project meteorologist in directing the aircraft through the reflectivity maxima were being relayed by voice from a distant radar site. Moreover, accurate aircraft positions were not available in real time to assist him in the precise vectoring of the penetrations.

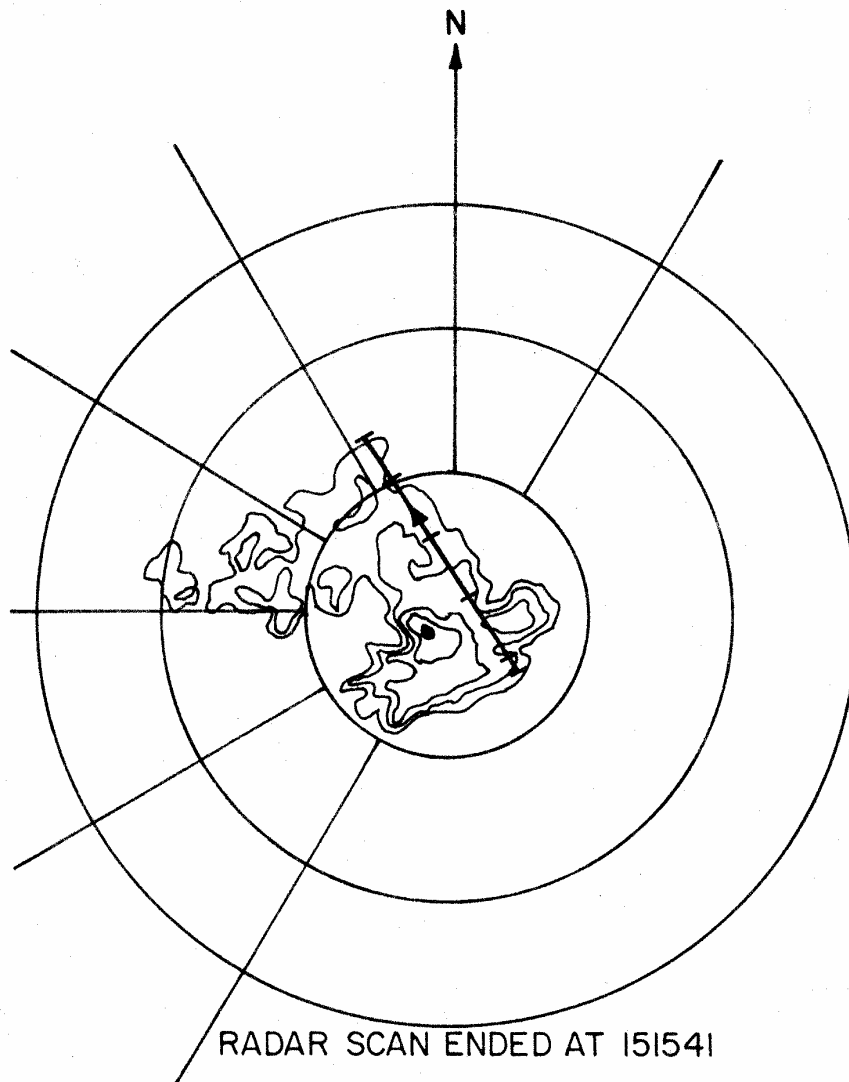


**Fig. 3:** T-28 track for Penetration 1 on 13 Aug 1978 superimposed on contoured slant range radar PPI presentation for approximate altitude and time of penetration. The threshold contour is 25 dBz with contour intervals of 10 dB. Shaded regions exceed 60 dBz. The cloud entry/exit times for the penetration were 151645/152041 EDT and the intervening tick marks correspond to clock times in whole minutes. The direction of penetration is indicated by the arrow on the track. The radials are at 30° intervals with true north as indicated. Range rings are at 10 km intervals.

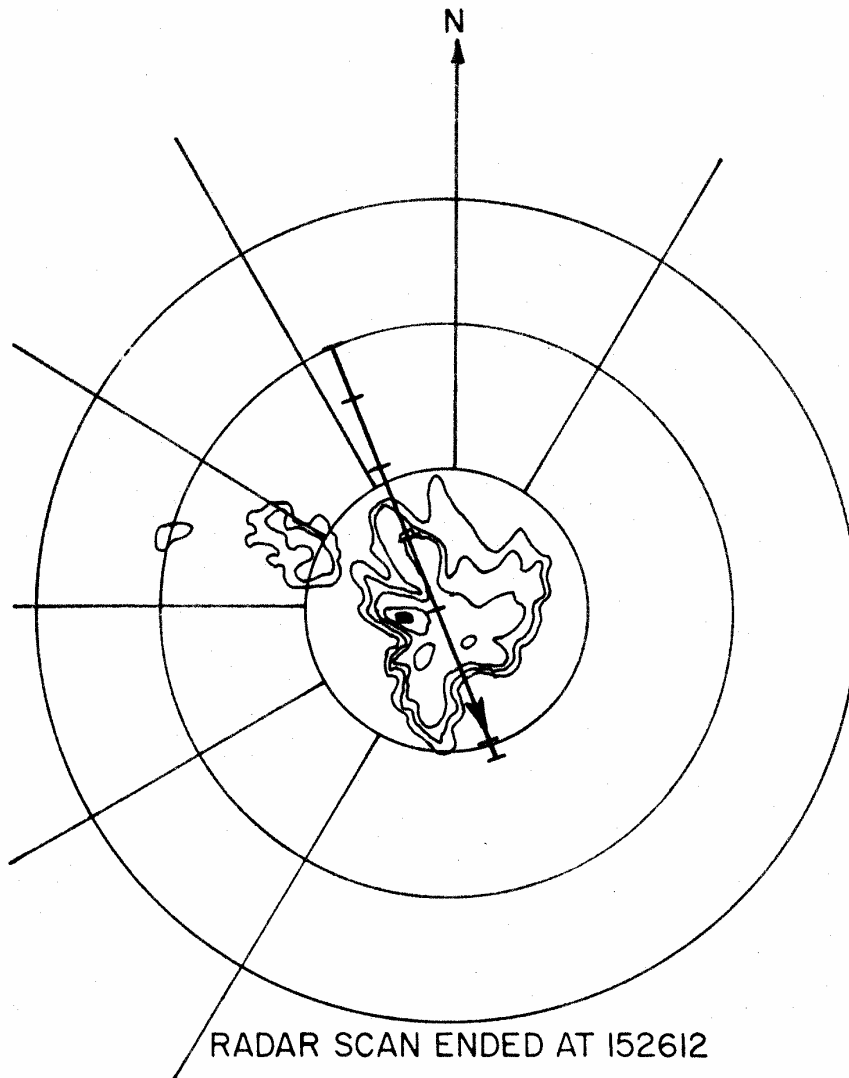


*Fig. 4:* Same as Fig. 3, except for Penetration 2 (152615-153216 EDT).

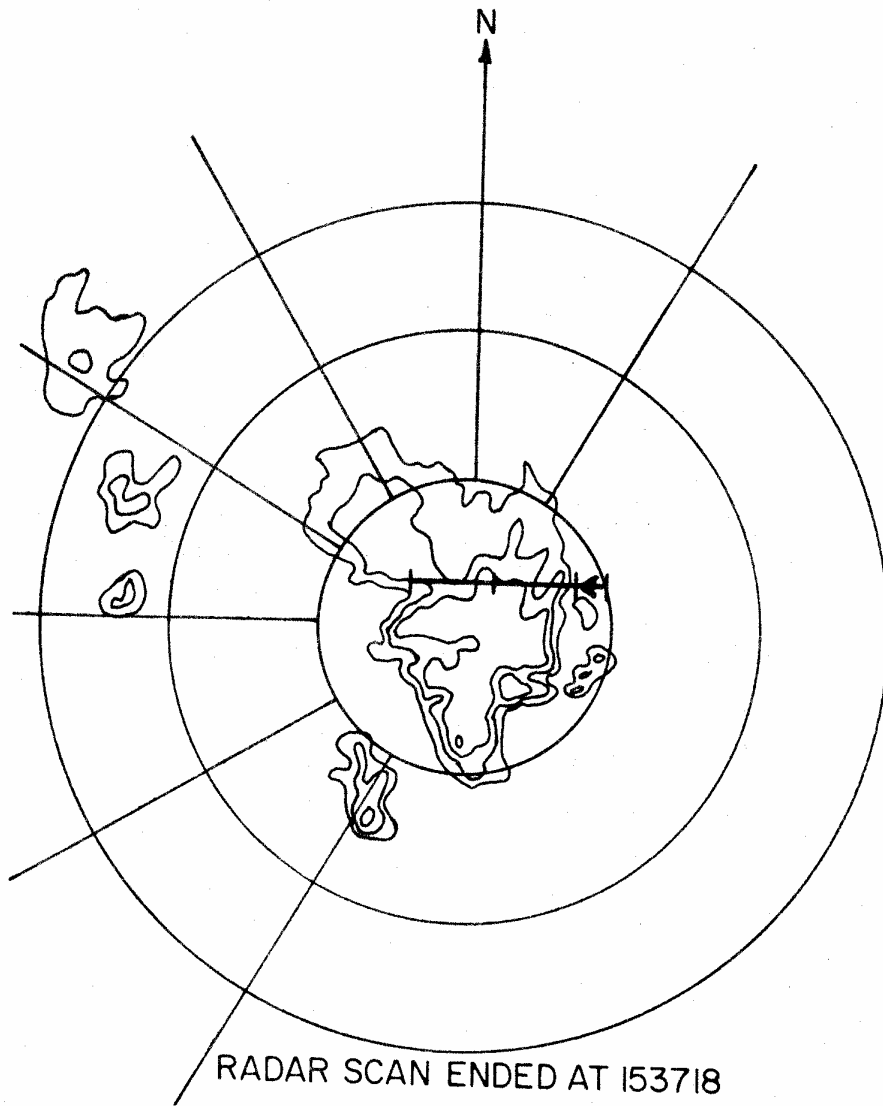
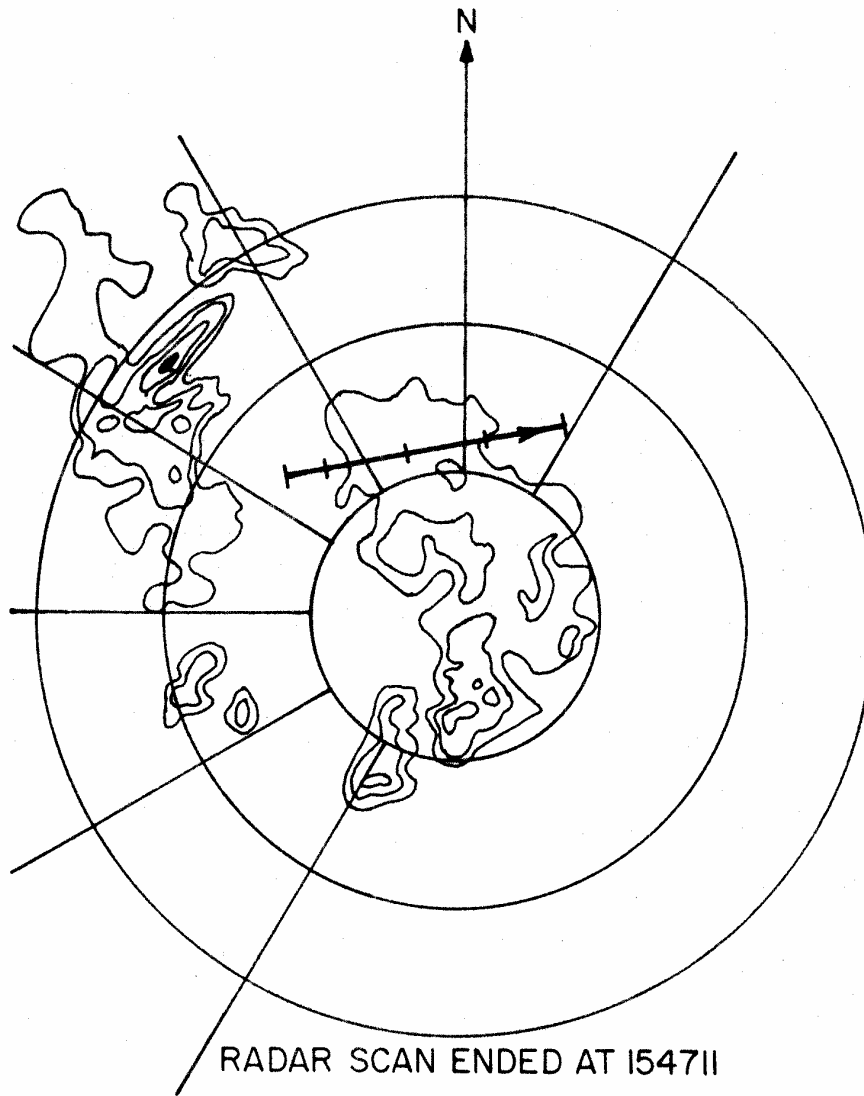
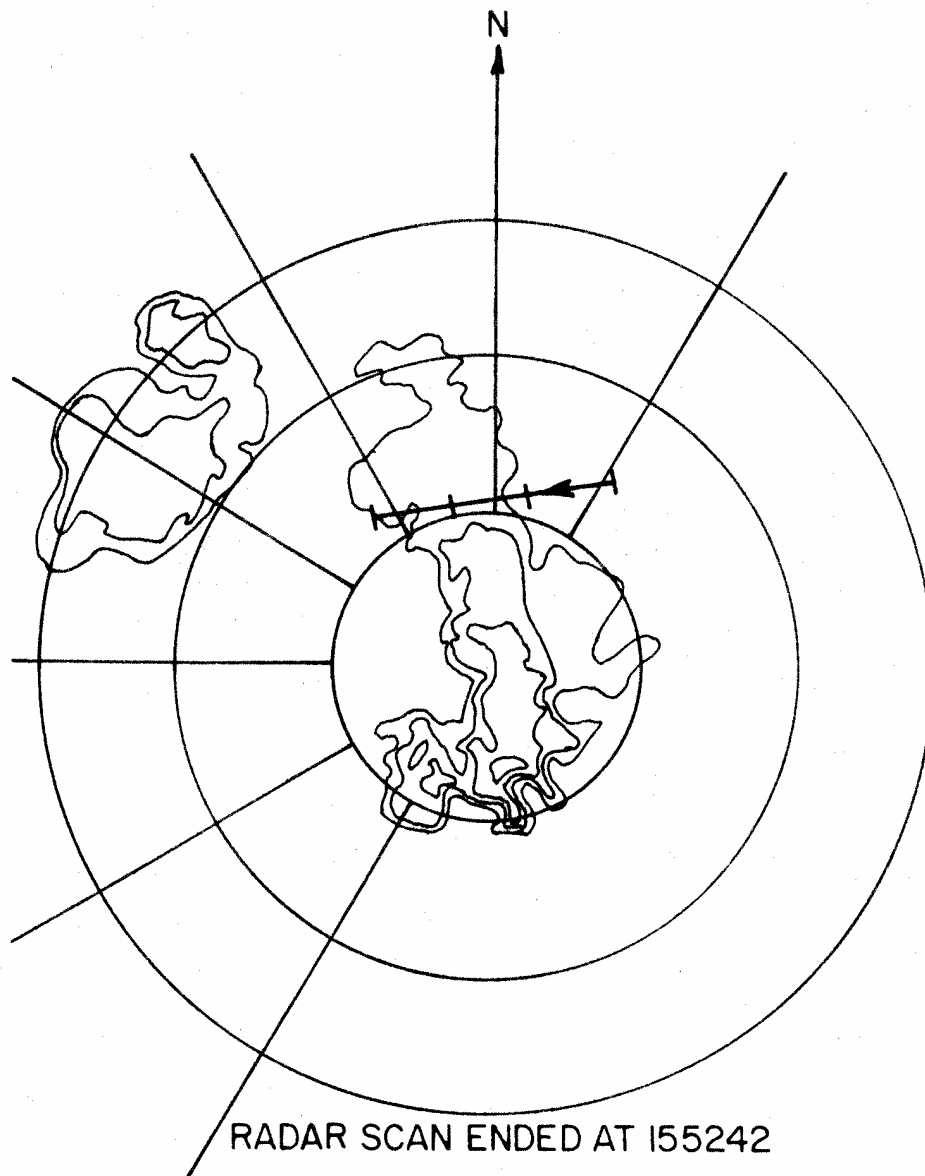


Fig. 5: Same as Fig. 3 except for Penetration 3 (153639-153900 EDT).



*Fig. 6:* Same as Fig. 3 except for Penetration 4 (154232-154600 EDT).



*Fig. 7:* Same as Fig. 3 except for Penetration 5 (154950-155309 EDT) and that threshold contour here is 15 dBz.

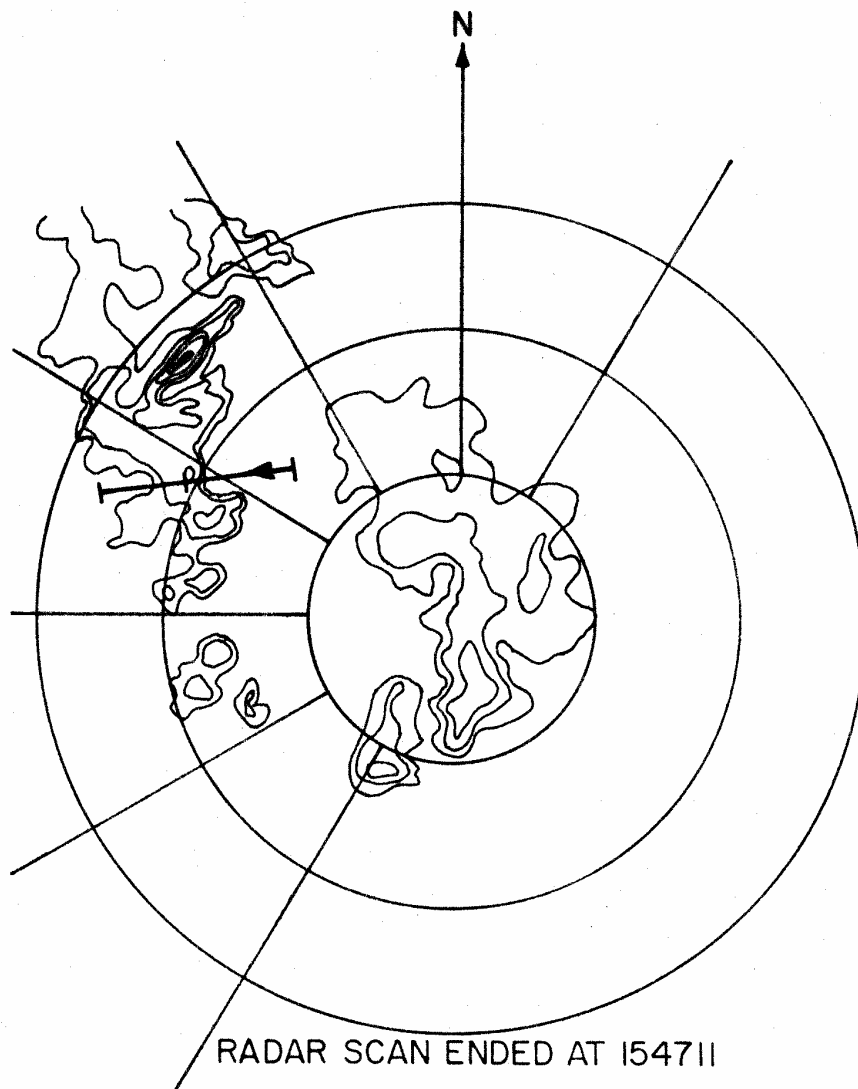


*Fig. 8:* Same as Fig. 3 except for Penetration 6 (155344-155602 EDT). Note that the radar scan sequence from which this figure was selected is the same as the one used for Fig. 6, and ended some 7 min prior to the penetration.



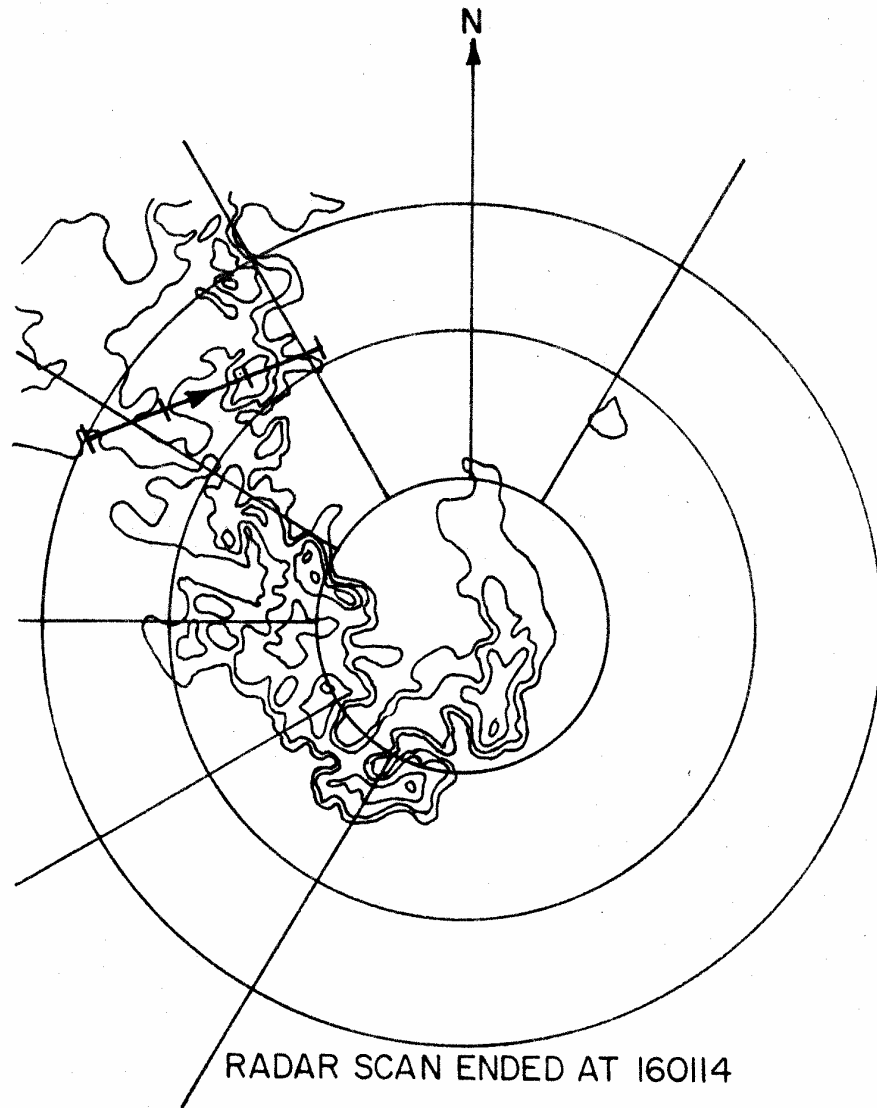


*Fig. 9:* Same as Fig. 3 except for Penetration 7 (155905-160155 EDT).

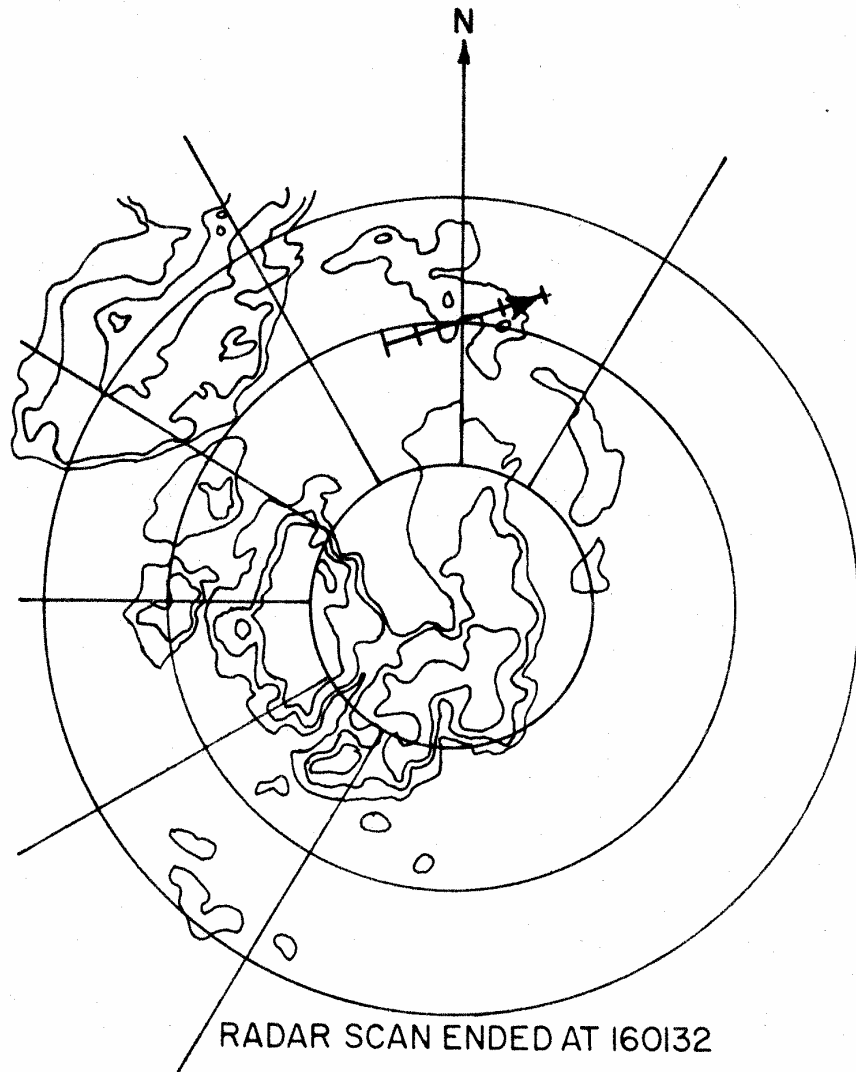


*Fig. 10:* Same as Fig. 3 except for Penetration 8 (160239-160429 EDT) and that threshold contour here is 15 dBz.

### 3.3 Hydrometeor Characteristics

#### 3.3.1 Cloud droplets

Figure 11 shows a typical cloud droplet spectrum observed by the PMS FSSP probe during Penetration No. 7 on 13 August. The measured spectra exhibit the typical broad range of droplet sizes characteristic of maritime clouds, but the observed cloud liquid water concentrations (LWC) were quite low. As noted in Sec. 2.3, low values were also measured with the J-W liquid water sensor, but the FSSP values of cloud LWC were typically two to four times the J-W values (Fig. 12). This behavior is consistent with the known tendency of the J-W instrument to underrepresent the contributions of cloud droplets larger than about 30  $\mu\text{m}$  in diameter (Spyers-Duran, 1968). In any case, the typical observed cloud liquid water concentrations were no more than 5 to 10% of the adiabatic values. In confirmation of the observed low cloud LWC, little aircraft icing was encountered during any of the storm penetrations.

The observed droplet number concentrations ranged up to a maximum of 350  $\text{cm}^{-3}$ , with typical values being about 200  $\text{cm}^{-3}$  in the updraft regions. The modal droplet size was usually around 15  $\mu\text{m}$  in diameter. The spectra suggest that some droplets larger than the upper size category of the T-28 FSSP (45  $\mu\text{m}$  in diameter) may have been present. It is also possible that the large diameter tails of the indicated droplet spectra could be due to ice particles; the response of the FSSP probe to small ice particles is not fully known.

#### 3.3.2 Ice particles observed by the PMS 2D probe

The hydrometeors larger than cloud droplets encountered during all the penetrations on 13 August appeared, from the 2D particle shadow images, to be mostly, if not entirely, ice. This interpretation is supported by the observations from the particle camera discussed in Sec. 3.3.3.

The raw 2D probe data were reviewed to obtain information about the ice crystal habits in the Florida clouds. The probe senses particles that range in size from 30  $\mu\text{m}$  up to more than 1000  $\mu\text{m}$ . However, shape recognition is practical only for particles with major dimensions of more than 100  $\mu\text{m}$ , and reliable only for ones larger than about 150  $\mu\text{m}$ . The difficulties with the PMS 2D system, mentioned in Sec. 2.4, resulted in the loss of approximately 40% of the 2D image data from the penetrations on 13 August. From the remaining images, it was determined that most of the recognizable ice particles during most of the penetrations were roughly spherical in nature, with occasional columns also present (Fig. 13). From a variety of evidence, some of which is discussed later, the nearly spherical particles are believed to be lightly rimed frozen raindrops. Occasional evidence of dendritic or aggregate-type particles also appeared in the data,

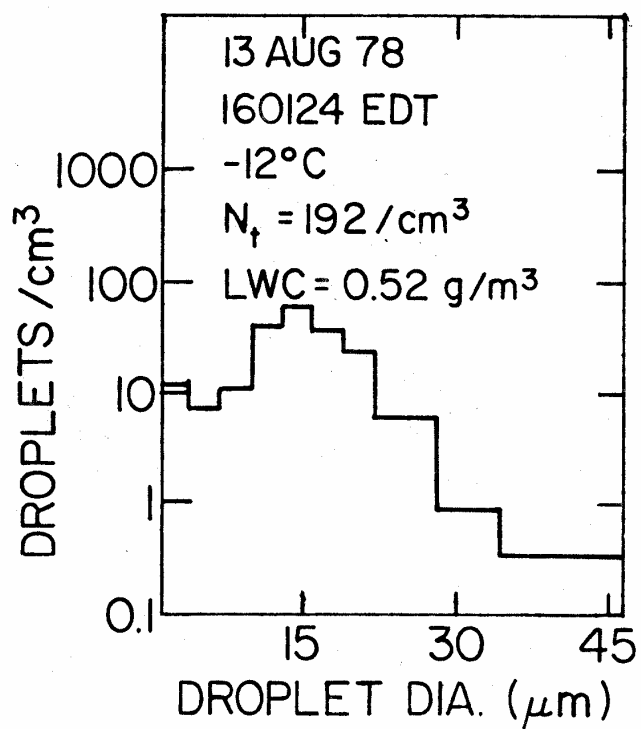


*Fig. 11:* A cloud droplet spectrum from an updraft region encountered during Penetration No. 7 on 13 Aug 1978.

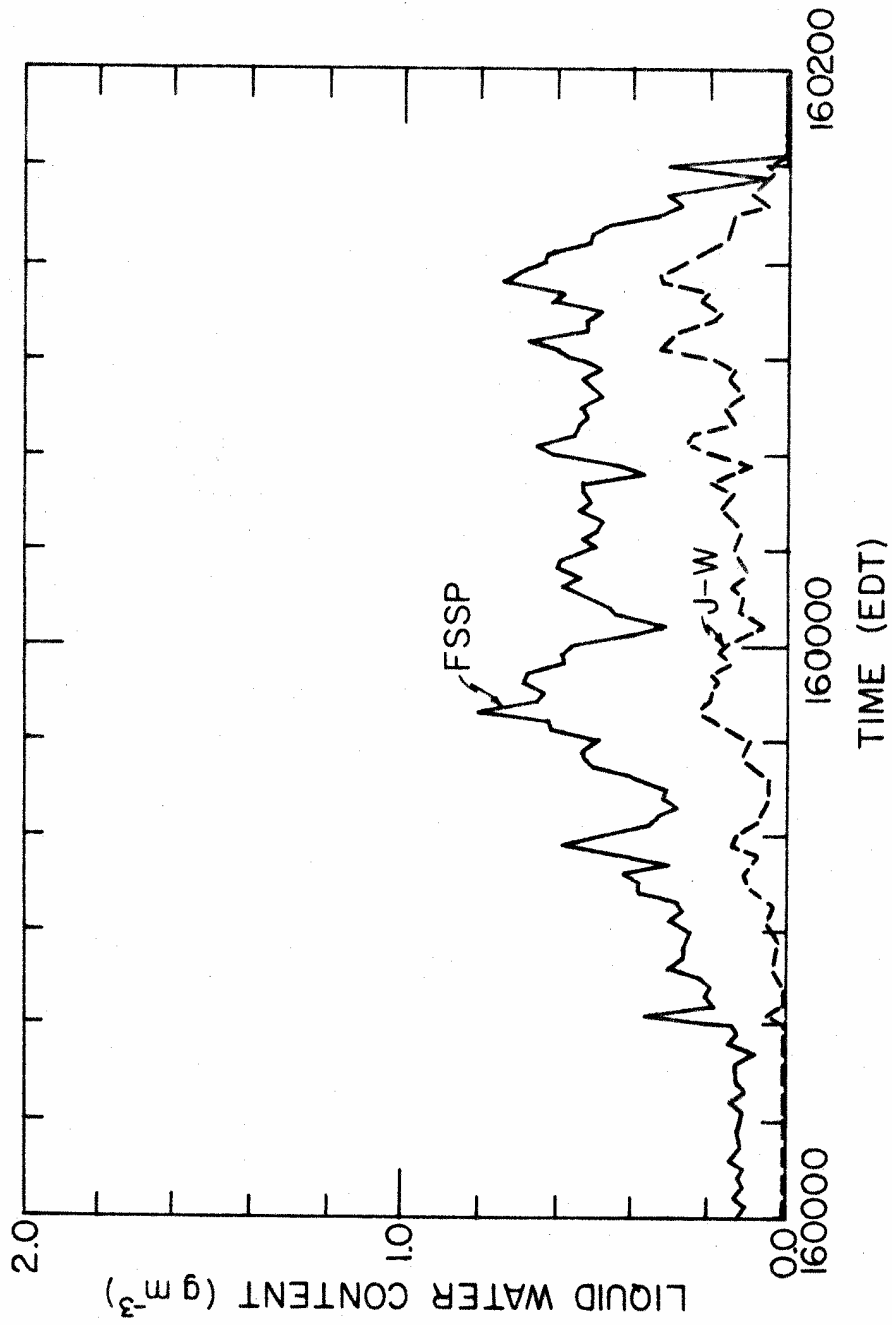


Fig. 12: Comparison of cloud liquid water concentrations measured by the PMS FSSP and the J-W sensor during part of Penetration No. 7 on 13 Aug 1978.

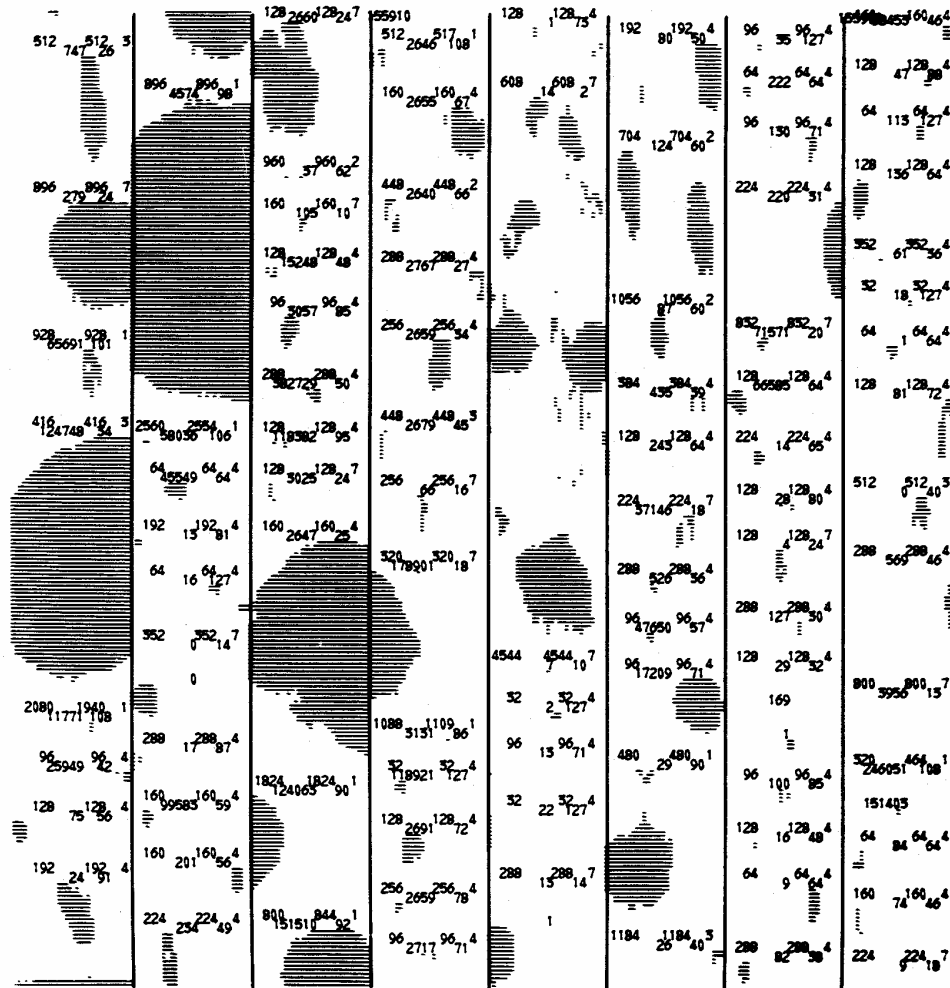


Fig. 13: Sample of PMS 2D probe particle image data from an updraft region of Penetration No. 7 on 13 Aug 1978. Distance between the horizontal bars corresponds to 1 mm. Most of the particles are graupel, apparently lightly rimed, or columns. Some examples of coincident particles passing through the optical array are evident.

especially during Penetration No. 8 (Fig. 14). This was the last penetration of the day and went through a storm in its dissipating stages.

Results from the numerical reduction procedures of Heymsfield and Parrish (1979) for the PMS 2D data indicate good agreement between the raw images and the numerically reduced data, as regards particle habits. Large variations occurred in the particle concentrations, as has also been observed in other locations. Typical total particle concentrations observed by the 2D probe were of the order of  $10^5 \text{ m}^{-3}$  in the regions of strong updrafts, with peak concentrations exceeding  $10^6 \text{ m}^{-3}$ . In the same updraft regions, the concentrations of precipitation-size particles (ones larger than  $500 \mu\text{m}$  in diameter) were of the order of  $10^3 - 10^4 \text{ m}^{-3}$ . These concentrations of the larger particles are rather high, but they are consistent with surface observations of raindrop concentrations in Florida. In regions of the clouds with little or no updraft, the corresponding number concentrations were usually approximately an order of magnitude smaller.

Mass concentrations were computed from the 2D probe data by assuming the particles to be ice with densities of about  $0.4 \text{ g cm}^{-3}$  (Heymsfield and Parrish, 1979). The resulting values were less than  $0.25 \text{ g m}^{-3}$  except during Penetration No. 7, where the maximum was about  $1.3 \text{ g m}^{-3}$ . The values obtained for Penetrations 1 through 3 were quite small ( $<0.1 \text{ g m}^{-3}$ ), but so many unusable 2D images occurred there that little confidence can be placed on the computations. The density values were based on observations of graupel particles from Colorado clouds, and the appearance of the Florida particles suggests that their densities may be higher. The limiting value for ice particles is  $0.9 \text{ g cm}^{-3}$ , so the mass concentrations might be up to twice the computed values (and probably more for Penetrations 1-3).

### 3.3.3 Precipitation particles

Figure 15 shows one frame from the particle camera data from Penetration No. 2 on 13 August,<sup>2</sup> illustrating the regular, approximately spherical, particles typically observed in the Florida storms. Liquid drops give dot pair images on the particle camera film (Fig. 22 shows an example of this). Thus the precipitation particles observed on 13 August, at temperatures between about  $-9^\circ\text{C}$  and  $-16^\circ\text{C}$ , were all ice. The largest particle in Fig. 15 is about  $2.5 \text{ mm}$  in diameter. Figure 16 shows a frame from Penetration No. 1 illustrating the same general particle characteristics, but the largest particle

---

<sup>2</sup>Unfortunately the particle camera ran out of film during Penetration No. 6, so no data are available for Penetration No. 7.

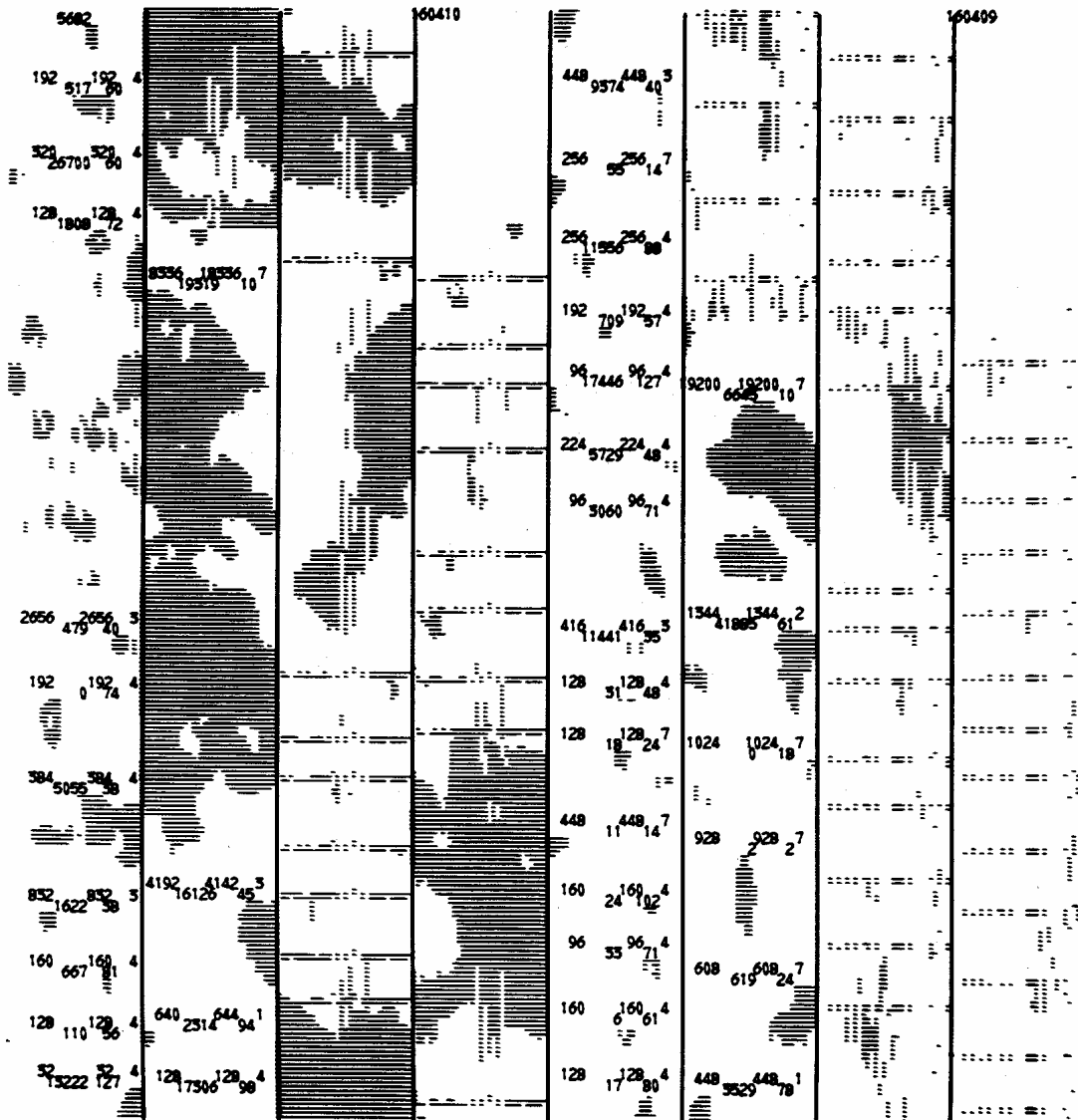


Fig. 14: Example of dendritic or aggregate particles observed by the PMS 2D probe during Penetration No. 8 on 13 Aug 1978.



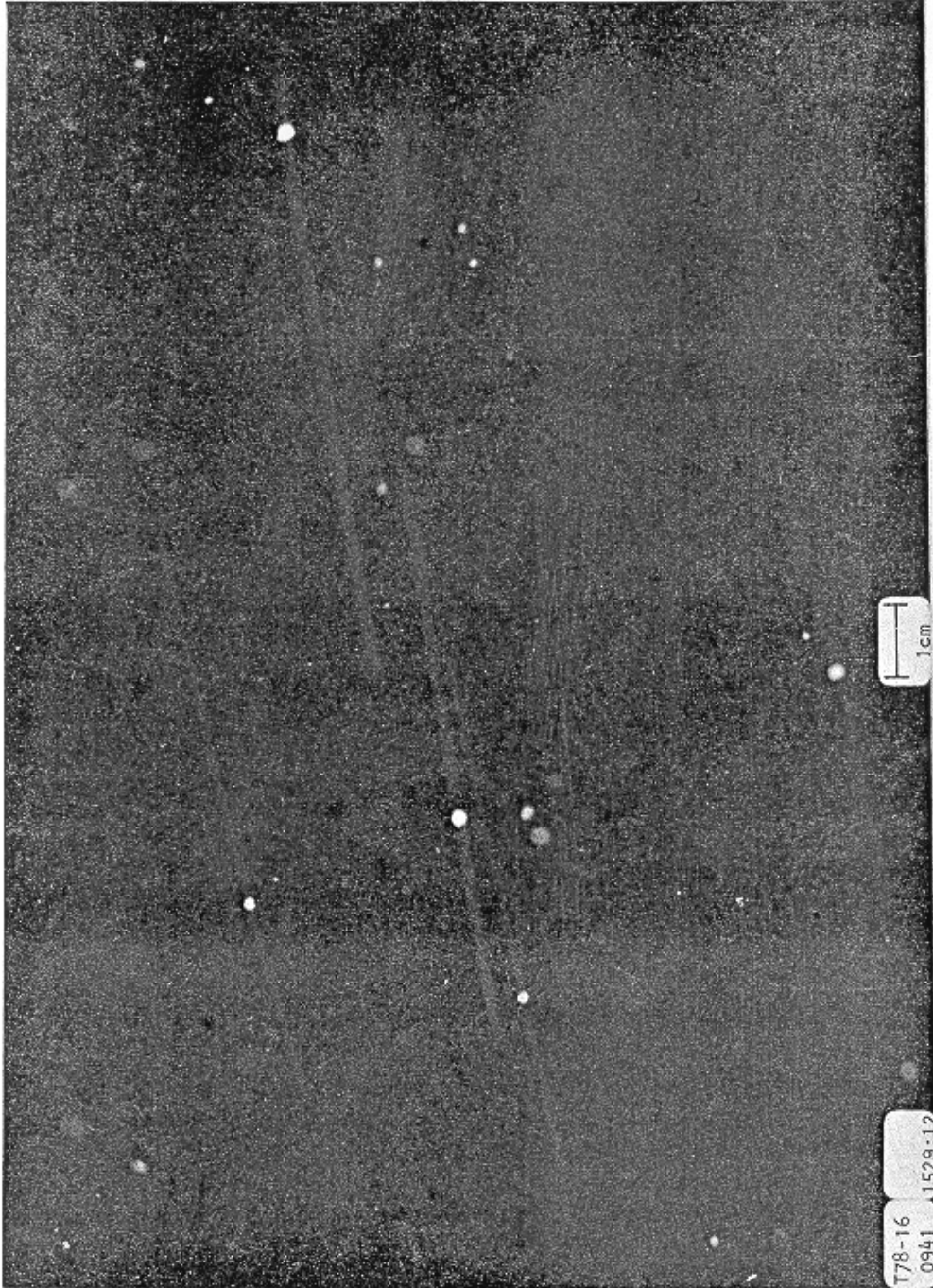


Fig. 15: Particle camera frame from Penetration No. 2 on 13 Aug 1978, showing nearly spherical ice particles in a weak downdraft at  $-11^{\circ}\text{C}$ .



*Fig. 16:* Particle camera frame from Penetration No. 1 on 13 Aug 1978, showing nearly spherical ice particles in an updraft of about  $6 \text{ m s}^{-1}$  at  $-11^{\circ}\text{C}$ .

in that figure is about 3 to 4 mm in diameter. The appearance of these precipitation-sized ice particles, nearly spherical in shape, suggests that they are frozen raindrops with light riming.

The foil impactor data were reviewed to estimate sample precipitation particle concentrations and sizes at various points. Only particles 1 mm in diameter or larger are normally considered in reducing the T-28 foil data, because of known problems with the foil impactor data for smaller sizes. The general impression one gains from cursory examination of the foil is of large concentrations of particles more or less regular in shape and all a few millimeters in diameter. The maximum concentrations on 13 August were about 500 particles per cubic meter, in the updraft regions of Penetration No. 6. This value is somewhat smaller than the corresponding particle concentrations from the PMS 2D probe, but those included particles down to 0.5 mm in diameter. Particles up to a maximum diameter of about 4 mm were found in the foil data, with the largest particles encountered on Penetrations 6 and 7. The particle imprints on the foil also suggest that the particles were ice, although the foil impactor is not a good instrument for making phase determinations (Knight *et al.*, 1977).

In summary, there is reasonable agreement among the precipitation particle observations made with the various instruments on the T-28. The particles observed on 13 August were essentially all ice and roughly spherical in shape, with small amounts of riming indicated. Although the particle habits are different, the number concentrations are generally similar to those observed in other regions of the country with the T-28. The maximum concentrations of precipitation particles were, however, higher than those found in clouds of the High Plains.

#### 3.4 Updraft and Thermodynamic Data

Plots of various measured and computed thermodynamic and related variables are given as functions of time for Penetrations 1, 2, 3, 6, and 7 on 13 August in Figs. 17-21. The first two penetrations went through moderately active regions of a storm right over the TICO Airport. The main updraft area on Penetration No. 1 (Fig. 17) was nearly 4 km wide, with maximum updraft speed near  $10 \text{ m s}^{-1}$ . (The irregularity of the updraft traces in Figs. 17-21 is due to inadequate smoothing of the altitude derivative, and causes the peak updraft speeds to be somewhat overestimated.) The computed equivalent potential temperature  $\theta_e$  reached  $344^\circ\text{K}$  in that updraft. Some other minor updraft areas are also apparent in the plot.

Three updraft areas were encountered on Penetration No. 2 (Fig. 18), with the widest being about 3 km wide and the strongest reaching a speed near  $15 \text{ m s}^{-1}$ . The buoyancy in the latter updraft reached about  $2.5^\circ\text{C}$ , with  $\theta_e$  values up to  $346^\circ\text{K}$ . The updrafts in Penetration No. 3 were weak (Fig. 19), but extended over a considerable distance.

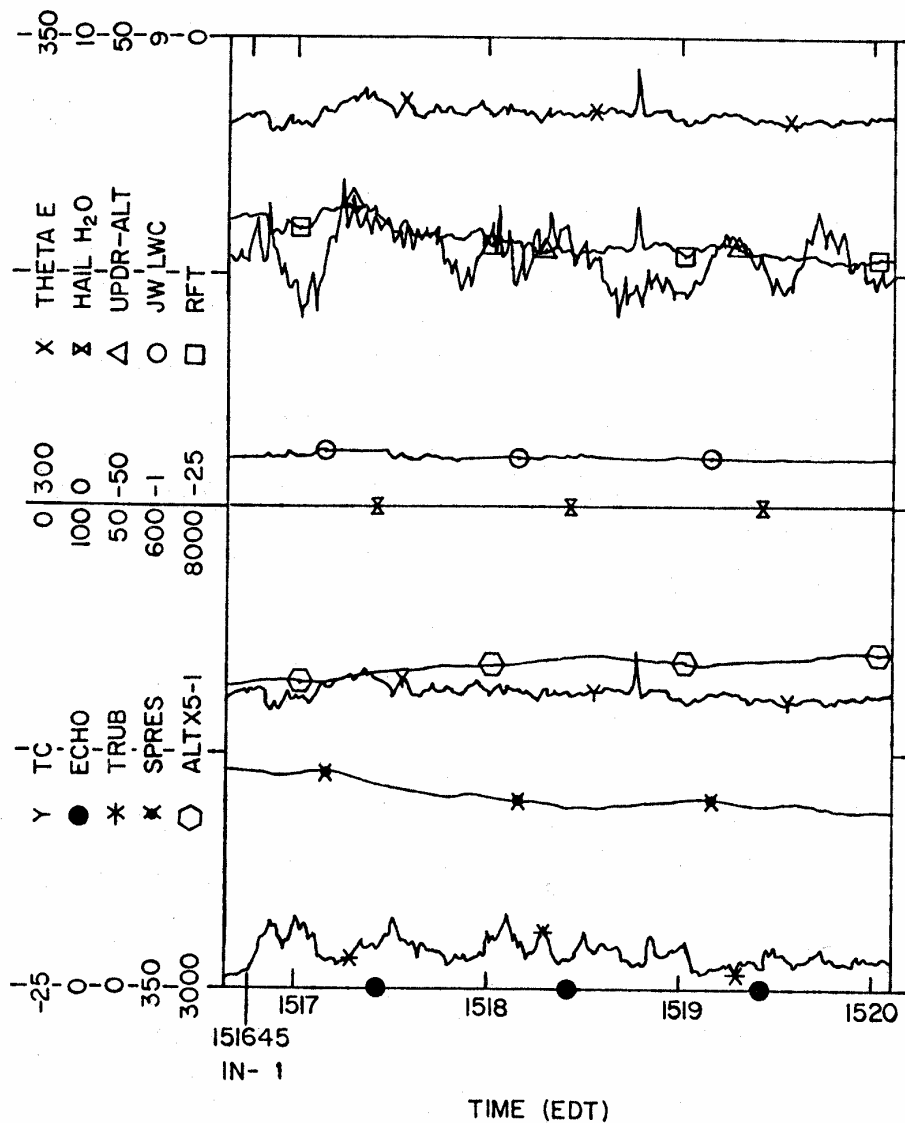


Fig. 17: Plot of measured and computed variables vs. time for most of Penetration No. 1 on 13 Aug 1978. Time scale on abscissa can be converted to an approximate distance scale by using the nominal T-28 flight speed of 6 km/min. Scales on ordinate indicate variables, plotting symbols, and scale ranges; key as follows: THETA E: Equivalent potential temperature ( $^{\circ}\text{K}$ ); HAIL  $\text{H}_2\text{O}$ : Hail mass concentration ( $\text{g}/\text{m}^3$ , always zero here); UPDR-ALT: Updraft speed ( $\text{m}/\text{s}$ ); JW LWC: Cloud liquid water concentration ( $\text{g}/\text{m}^3$ ); RFT: Temperature ( $^{\circ}\text{C}$ ); TC: Temperature adjusted for altitude changes ( $^{\circ}\text{C}$ ); ECHO: Radar reflectivity factor due to hail ( $\text{dBz}$ , always zero here); TRUB: Turbulence  $\varepsilon^{1/3}$  ( $\text{cm}^2/3\text{s}^{-1}$ ); SPRES: Static pressure ( $\text{mb}$ ); and ALTX5-1: Pressure altitude ( $\text{m}$ ).

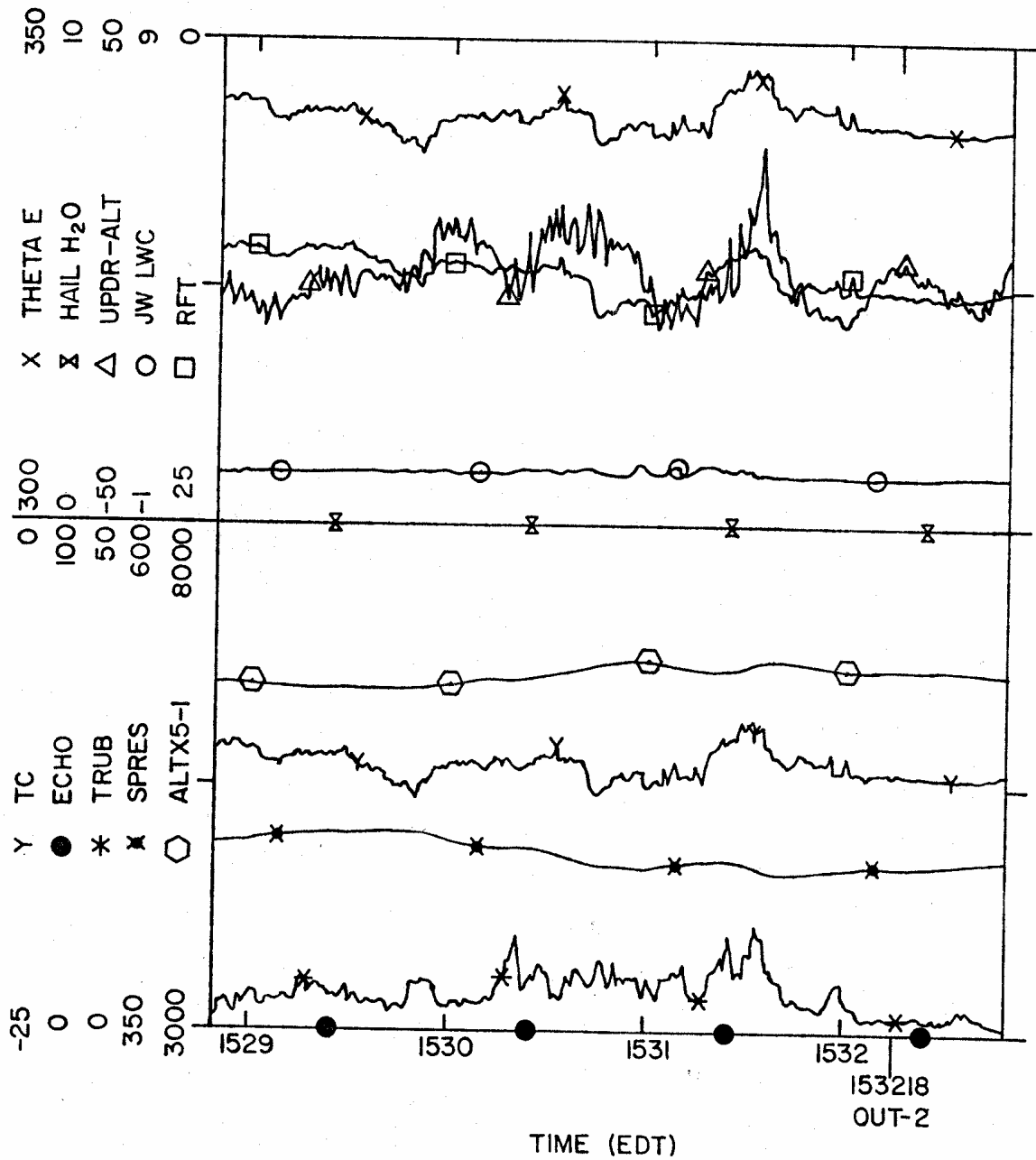


Fig. 18: As Fig. 17, but for the portion of Penetration No. 2 on 13 Aug 1978 containing significant updrafts.

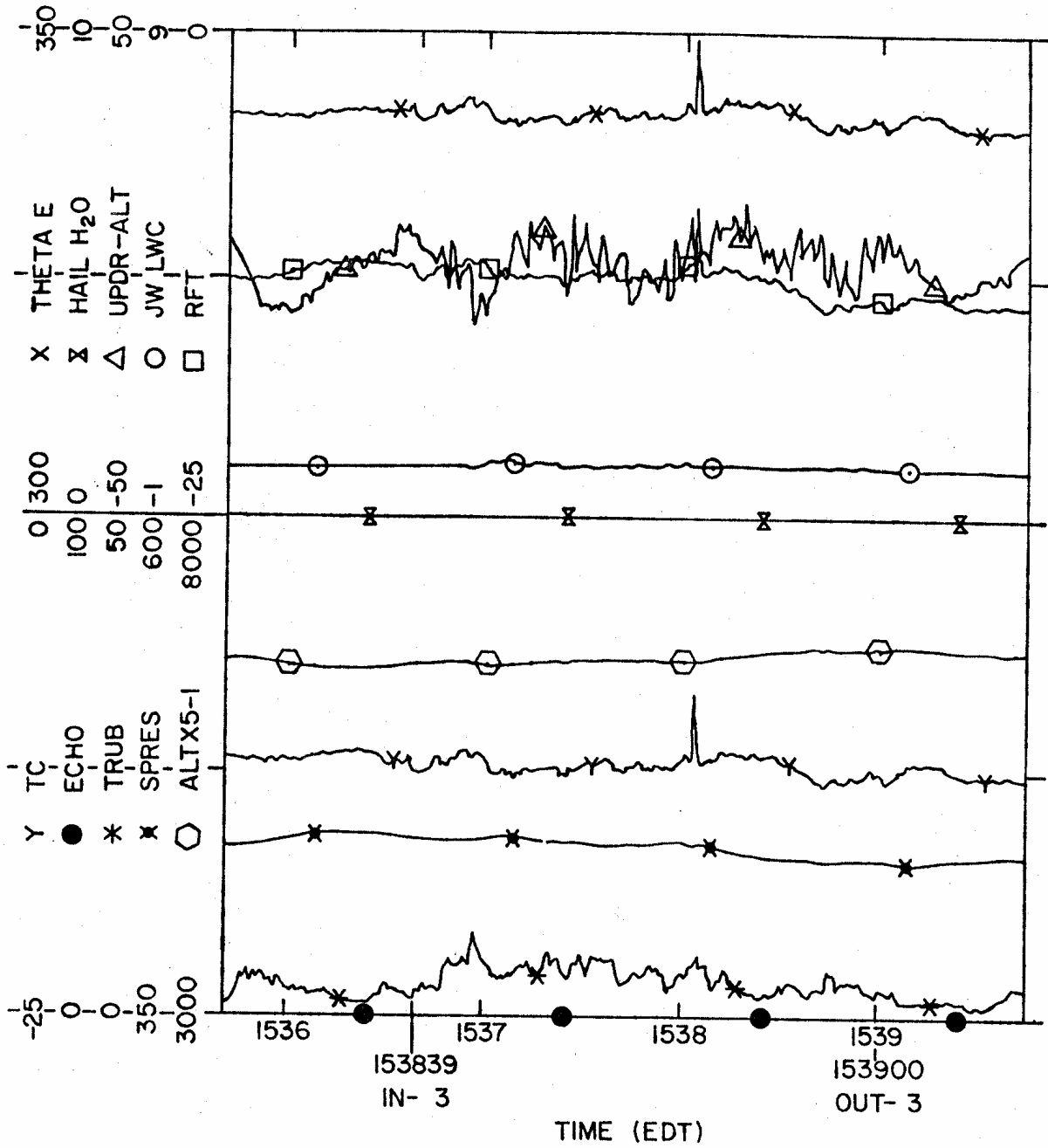


Fig. 19: As Fig. 17, but for Penetration No. 3 on 13 Aug 1978.

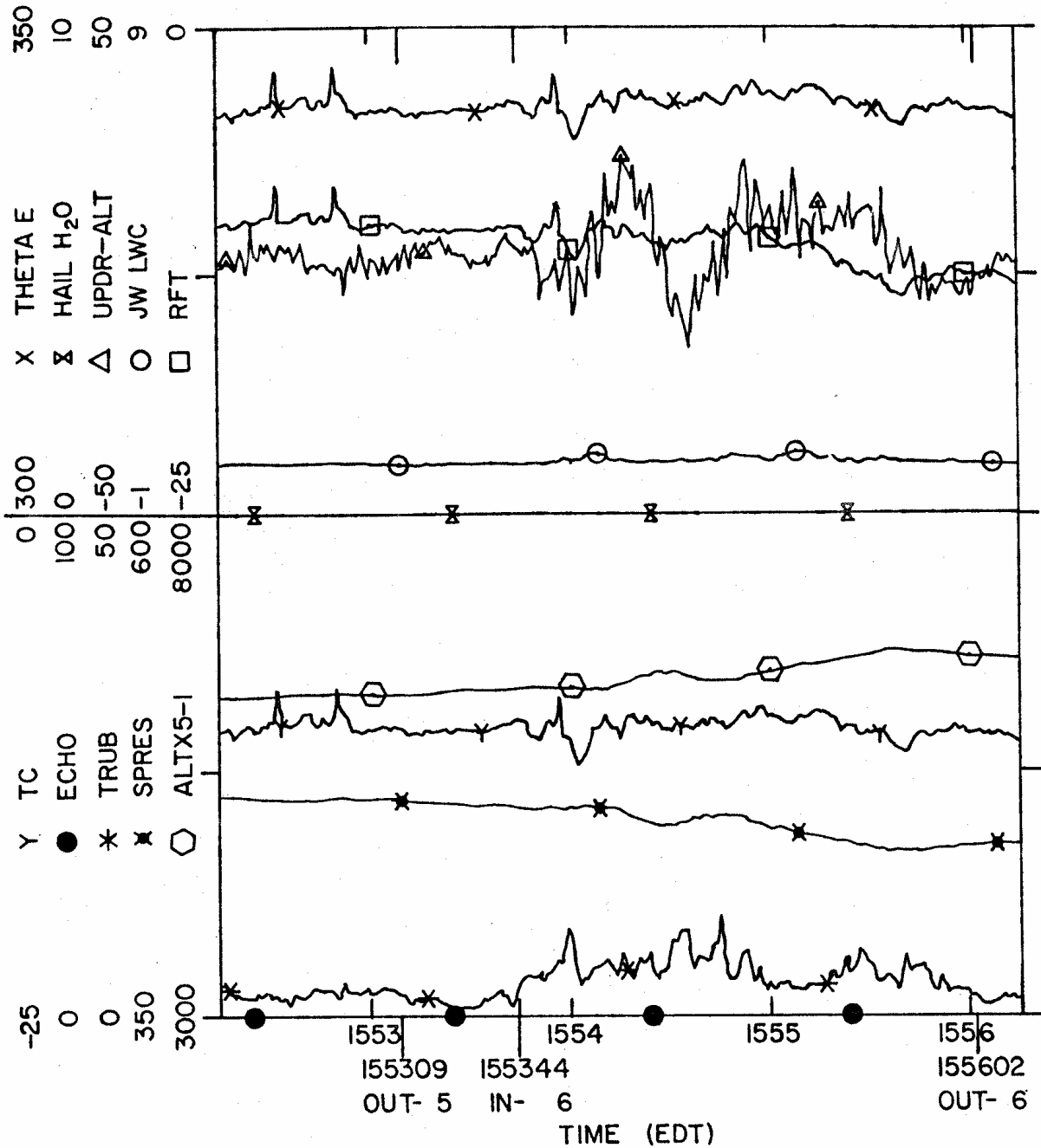


Fig. 20: As Fig. 17, but for Penetration No. 6 on 13 Aug 1978.

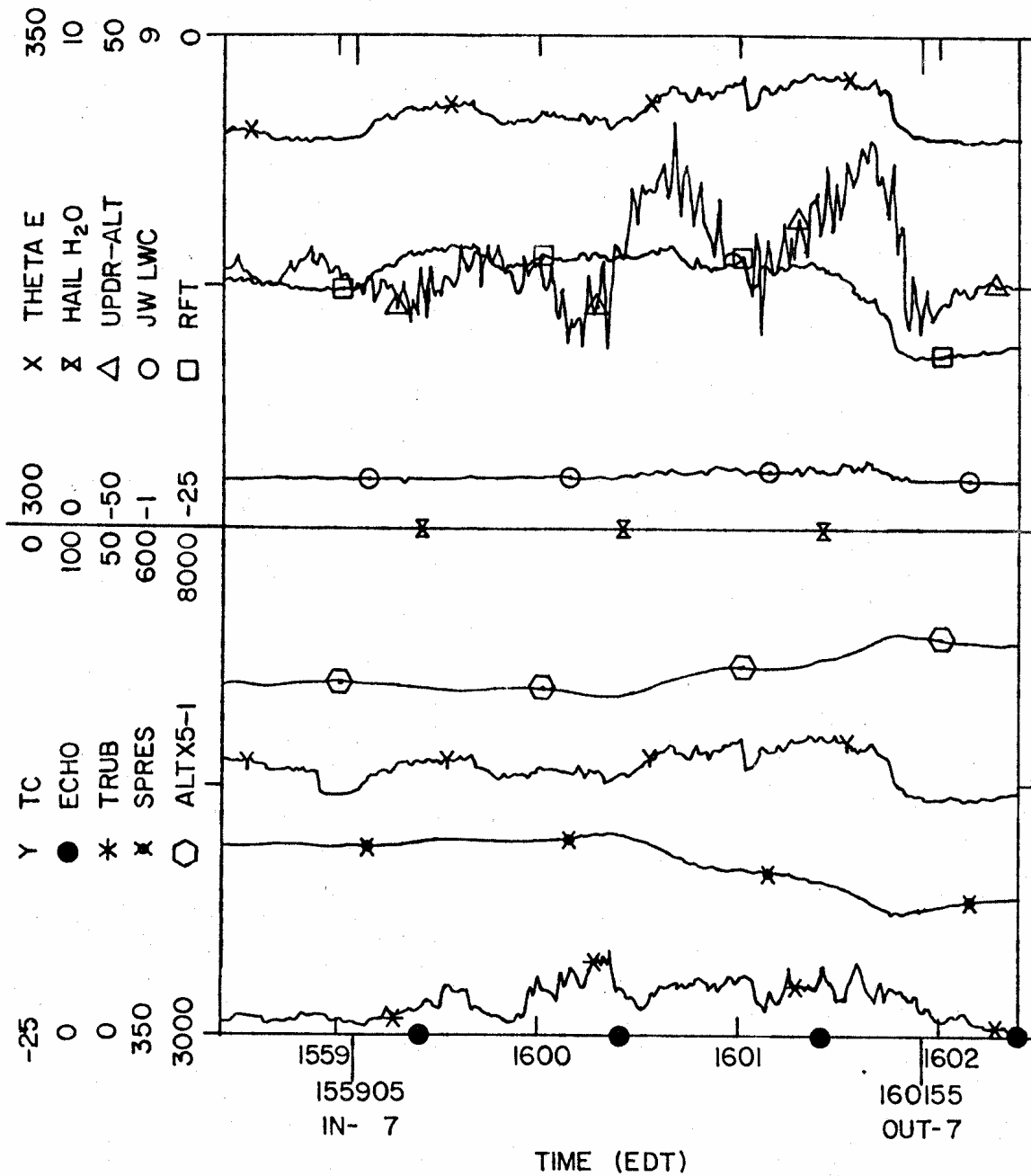


Fig. 21: As Fig. 17, but for Penetration No. 7 on 13 Aug 1978.



No plots are shown for Penetrations 4 and 5, because they passed through fringe areas of the storm and no significant updraft areas were encountered. Penetrations 6 and 7 passed through a different storm, to the west of the one studied previously. Two main updraft areas were found on Penetration No. 6 (Fig. 20), with a narrow downdraft in between. The first updraft was about 2 km wide and the second about 4 km wide, with maximum updrafts of more than  $12 \text{ m s}^{-1}$  in each. There were also two major, but nearly contiguous, updrafts in Penetration No. 7 (Fig. 21); each was about 3-4 km wide. The updraft speeds reached about  $15 \text{ m s}^{-1}$  in the first and about  $20 \text{ m s}^{-1}$  in the second. Buoyancy values in the second ranged up to about  $3^\circ\text{C}$ , and  $\theta_e$  reached  $345^\circ\text{K}$ .

No plot is shown for Penetration No. 8, because it passed through the decaying portion of a third storm and no updrafts were found.

### 3.5 Disposition of Condensed Water in the Clouds

The fact that the cloud liquid water concentrations observed in all T-28 penetrations of the Florida clouds were quite small raises a question concerning the disposition of the condensed cloud liquid. To investigate this question, peak values of hydrometeor mass concentrations were obtained from the PMS FSSP probe, the PMS 2D probe, and the foil impactor. The concentrations determined from the foil impactor data are based on spot checks and must be considered as estimates. The peak mass concentrations from each device for each penetration were summed to establish an upper bound for the total condensed water concentration for each penetration on 13 August. These extremes were then compared with the appropriate adiabatic values, with the results given in Table 4.

The ratios of the "upper bounds" on the total water concentrations to the adiabatic concentrations ranged from less than 0.05 to about 1.0. Thus even after summing the (not necessarily coincident in space) peak mass concentrations for each penetration, the ratios are still considerably less than one except for Penetration No. 7. The ratio tends to be higher for the penetrations that came closer to the storm reflectivity maxima. In Penetration No. 7, the aircraft passed right through the maximum reflectivity and the total condensed water concentration comes very close to the adiabatic value. The ratio of total observed to adiabatic condensed water concentration also tends to be higher in the penetrations that went through reasonably well defined updrafts (Nos. 1, 2, 6, and 7), suggesting the importance of the updraft to the precipitation process.

Although the FSSP probe senses hydrometeors of cloud droplet sizes, questions exist concerning the accuracy of the instrument. There is some evidence that the indicated cloud LWC may be low, perhaps by as much as a factor 2. The mass concentrations computed from the PMS 2D

TABLE 4

Comparison of Hydrometeor Mass Concentrations  
Observed on 13 Aug 1978 with Adiabatic Values

Pen. No.	Cloud <sup>1,2</sup> LMC (FSSP) [g m <sup>-3</sup> ]	Embryos <sup>1,3</sup> (2D Probe) [g m <sup>-3</sup> ]	Precipitation <sup>1,5</sup> Particles (Foil) [g m <sup>-3</sup> ]	Total Mass Concentration [g m <sup>-3</sup> ]	Adiabatic LMC [g m <sup>-3</sup> ]	Ratio of Total to Adiabatic
1	0.7	0.01 <sup>4</sup>	1-2	1.7-2.7	7.8	0.22-0.35
2	1.1	0.09 <sup>4</sup>	2-4	3.2-5.2	7.9	0.40-0.66
3	0.7	-- <sup>4</sup>	1.5	2.2	7.9	0.28
4	0.1	0.14	0.5	0.7	7.9	0.09
5	0.1	0.09	0.2	0.4	7.6	0.05
6	1.0	0.24	1-2	2.2-3.2	7.9	0.28-0.40
7	0.8	1.3	4-6	6.1-8.1	7.9	0.77-1.02
8	0.1	0.15	-- <sup>6</sup>	0.2	7.9	0.02

<sup>1</sup>peak value observed during entire penetration.

<sup>2</sup>Accuracy suspect; values may be low by up to a factor 2.

<sup>3</sup>Based on particle densities of about 0.4 g cm<sup>-3</sup> determined for graupel in Colorado clouds. Florida particles appeared to be frozen raindrops, so values could be up to twice as large.

<sup>4</sup>Most 2D image data unusable; only rough estimates possible.

<sup>5</sup>Estimates based on spot samples from selected portions of foil with high concentrations and/or large particles. Density taken as 1 g cm<sup>-3</sup>.

<sup>6</sup>All particles apparently < 0.5 mm diameter.

probe data are also likely to be low because the analysis assumed particle densities of about  $0.4 \text{ g cm}^{-3}$ . Thus the overall total hydrometeor mass concentrations given in Table 4 are likely to be too low. Allowing for this factor would make the total condensed water concentrations in the penetrations through active parts of the storms (Nos. 1, 2, 6, and 7) approach adiabatic values, and perhaps even exceed the adiabatic value for No. 7. In the other cases, the adjusted values would still be lower than one, but fall out of the precipitation associated with the rapid life cycles of Florida clouds could easily account for those observations. If each penetration had passed through the right place at the right time for each cloud, it is likely that all the ratios would be near one.

The fact that the precipitation-size particles dominate the total mass concentration in each case suggests that the Florida clouds are very efficient in converting water from cloud droplets to precipitation-size particles. The clouds grew and decayed very quickly, with practically no anvils present, on the days of the T-28 penetrations. These visual observations, plus the fact that the total condensed water concentrations tended to approach the adiabatic values in regions of high radar reflectivity, suggest that the water is processed very efficiently in the Florida clouds. There is no evidence from these observations of any storage or accumulation mechanism in the clouds.

#### 4. OBSERVATIONS ON OTHER RESEARCH DAYS

The aircraft data gathered on the other research days have not been analyzed in the same detail as the 13 August data discussed in Section 3. The limited information from those other days presented here has been selected primarily to supplement or contrast with the observations from 13 August. A discussion of all the observations as they relate to possible precipitation or electrification mechanisms is presented in Section 5.

##### 4.1 Data from 9 August 1978

Some of the more interesting T-28 observations occurred on this day. The penetrations were made through mid-afternoon mature thunderstorms at altitudes corresponding to relatively warm parts of the supercooled cloud region. The measured in-cloud temperatures ranged from about  $-3^{\circ}\text{C}$  to  $-10^{\circ}\text{C}$ . The conditions were generally similar to those on 13 August, except that the flight altitude was lower and the temperatures higher. This makes comparison of the 9 August data with those from 13 August of particular interest.

The basic T-28 meteorological data for 9 August are good, as are the particle camera data. Unfortunately, the storms on that day were well to the west of KSC, outside the TRIP area instrumented for intensive study. They were also beyond the range of the KSC X-band radar, so only voice relayed maximum radar reflectivity factors were available to aid the project meteorologist in directing the penetrations. Examination of computed equivalent potential temperatures for the flight suggests that only Penetration No. 6 passed through the most active updraft region of a storm. Only limited supporting TRIP data are available for 9 August, and no recorded radar data were accessible for analysis. Moreover, the decision to investigate the storms at that distance was taken rather suddenly and the control switch for the PMS equipment was inadvertently left off so that no PMS data exist for this flight. The foil impactor data were good but were not analyzed in detail.

The observations from Penetration No. 6 on 9 August are of particular interest. High concentrations of supercooled raindrops were found in the main updraft region of the storm. The presence of liquid drops is indicated by dot-pair images on the particle camera film, as illustrated in Fig. 22. That frame shows raindrops in a concentration of the order of  $500\text{ m}^{-3}$  in an updraft of  $16\text{ m s}^{-1}$  where the temperature was  $-5^{\circ}\text{C}$ . No ice particles are evident, and the J-W cloud liquid water concentration at that location was about  $0.4\text{ g m}^{-3}$ . The drop sizes can be determined from (and are approximately equal to) the spacings between the dots of each pair; the largest drop in Fig. 22 is about 3.5 mm in diameter.

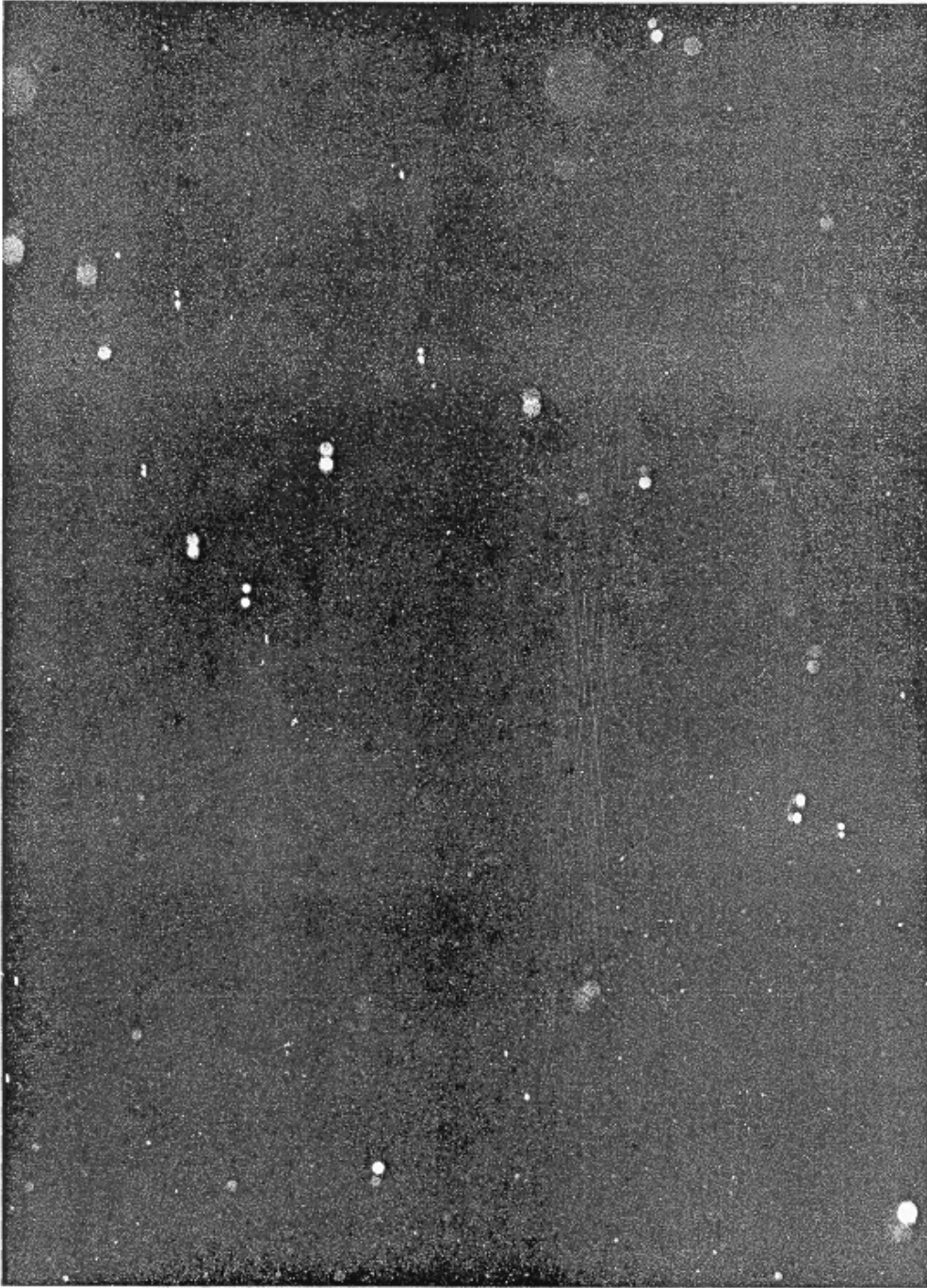


Fig. 22: Particle camera frame from Penetration No. 6 on 9 Aug 1978, showing liquid raindrops in an updraft of about  $16 \text{ m s}^{-1}$  at a temperature of about  $-5^\circ\text{C}$ .

These observations suggest that the cloud was very efficient in converting condensed water into precipitation-sized particles. Because the raindrops were observed in an updraft at temperatures around  $-5^{\circ}\text{C}$ , it is reasonable to infer that they formed by coalescence lower down in the warmer part of the cloud. During an earlier penetration (No. 1) of the same storm on 9 August, a mixture of liquid and frozen raindrops was found in a weak updraft (about  $5\text{ m s}^{-1}$ ) at temperatures around  $-7^{\circ}\text{C}$ . These observations, coupled with those on 13 August of nearly spherical millimeter-sized ice particles higher up in the storms (around  $-13^{\circ}\text{C}$ ), indicate that the raindrops form in the updraft region in the warm part of the cloud and then freeze in the  $-5^{\circ}\text{C}$  to  $-10^{\circ}\text{C}$  region. The distorted particle shapes noted on 13 August could be accounted for by light riming of the frozen raindrops.

The updraft during Penetration No. 6 on 9 August was about 5 km wide and very buoyant. A temperature excess of  $4 - 5^{\circ}\text{C}$  extended over a distance of more than 3 km, exactly coincident with the region of measurable (J-W) cloud liquid water. The maximum updraft speed was about  $21\text{ m s}^{-1}$ , the strongest found on that day, and the peak J-W cloud liquid water concentration of  $0.6\text{ g m}^{-3}$  was the highest observed on any T-28 flight in Florida. Observations of such strong buoyancy have been rare in the T-28 investigations of storms in the High Plains region.

#### 4.2 Data from 10 August 1978

The clouds on this day were weak towering cumulus with tops extending up to about 6.4 km (21,000 ft) MSL. The T-28 penetrations were made shortly after local noon and, as indicated in Table 2, all the clouds studied were small. The penetrations were again made through the relatively warm part of the supercooled cloud region, with measured temperatures ranging from  $-6^{\circ}\text{C}$  to  $-10^{\circ}\text{C}$ . The maximum updraft speed encountered on 10 August was  $12\text{ m s}^{-1}$  and the downdraft speed usually exceeded the updraft. The cloud liquid water concentrations were also low for every penetration.

It is of some interest to note that the strongest turbulence found in the T-28 Florida flights occurred on 10 August, during Penetration No. 8. Values of the turbulent eddy dissipation rate  $\epsilon$  are determined from the T-28 data by Fourier analysis of the indicated airspeed data (Kyle et al., 1976). The computed values for  $\epsilon$  near the edge of the  $12\text{ m s}^{-1}$  updraft approached  $2000\text{ cm}^2\text{ s}^{-3}$ . Even this maximum is small compared to observations from storms of the High Plains, where  $\epsilon$  sometimes reaches values 10 times as large. The rather modest values of  $\epsilon$  for the Florida clouds may suggest that entrainment from the sides plays a limited role in the cloud evolution.

As is reasonable for such small clouds, the total particle concentrations determined from the PMS 2D probe data generally ranged between 1 and  $10 \ell^{-1}$  with maxima around  $30 \ell^{-1}$ . The concentrations of precipitation-sized particles (larger than 0.5 mm) ranged mostly between 100 and  $1000 \text{ m}^{-3}$ , with maxima around  $2000 \text{ m}^{-3}$ .

While the penetrations on 10 August were made at relatively high temperatures, the presence of liquid drops has not been ascertained because the particle camera data have not been reduced. Figure 23 shows a typical sample of the PMS 2D images for this day, from the updraft region on Penetration No. 5. Most of the particles are generally round, although they tend to be smaller than those observed on 13 August. The departures from spherical shape are sufficiently great that the particles are probably ice, but there is some suggestion in other PMS 2D probe data from 10 August that some of the particles may be liquid. Again, there were occasional particles which appear to be columns, and even some aggregates. Figure 24 shows examples of the latter, from a downdraft region of Penetration No. 2.

An interesting particle was observed during Penetration No. 9 on this day (Fig. 25). It resembles two spheres stuck together. The nearby particles are evidently ice, so it seems likely that this one is also ice. The particle appears to consist of two frozen raindrops, joined after one (or perhaps both) initially froze.

#### 4.3 Data from 12 August 1978

The T-28 made 18 cloud penetrations on this day, around local noon. During the early penetrations the clouds were in the towering cumulus stages, but they evolved to weak thunderstorms during the last several penetrations. The flight was made at relatively low temperatures, with the measured in-cloud temperatures ranging from  $-9^{\circ}\text{C}$  to  $-17^{\circ}\text{C}$ . The strongest updraft observed in Florida ( $23 \text{ m s}^{-1}$ ) occurred on this day, during Penetration No. 17 through a rather small turret. The observed cloud liquid water concentrations were again low.

Once again the particles observed by the PMS 2D probe showed a tendency toward nearly spherical shapes (Fig. 26), but they were distorted enough to be obviously ice rather than liquid. Figure 26 was taken from a region of weak updraft during Penetration No. 18. Some columnar particles were again present. There were also some instances of aggregate particles; Fig. 27 shows aggregates which appeared in a region of relatively neutral vertical motion during Penetration No. 5. The aggregates appeared to be several millimeters in size, while the "spheres" tended to be somewhat larger later in the flight corresponding to the observed change from towering cumulus clouds to weak thunderstorms. The particles observed toward the end of the 12 August flight were similar to the ones encountered on 13 August.

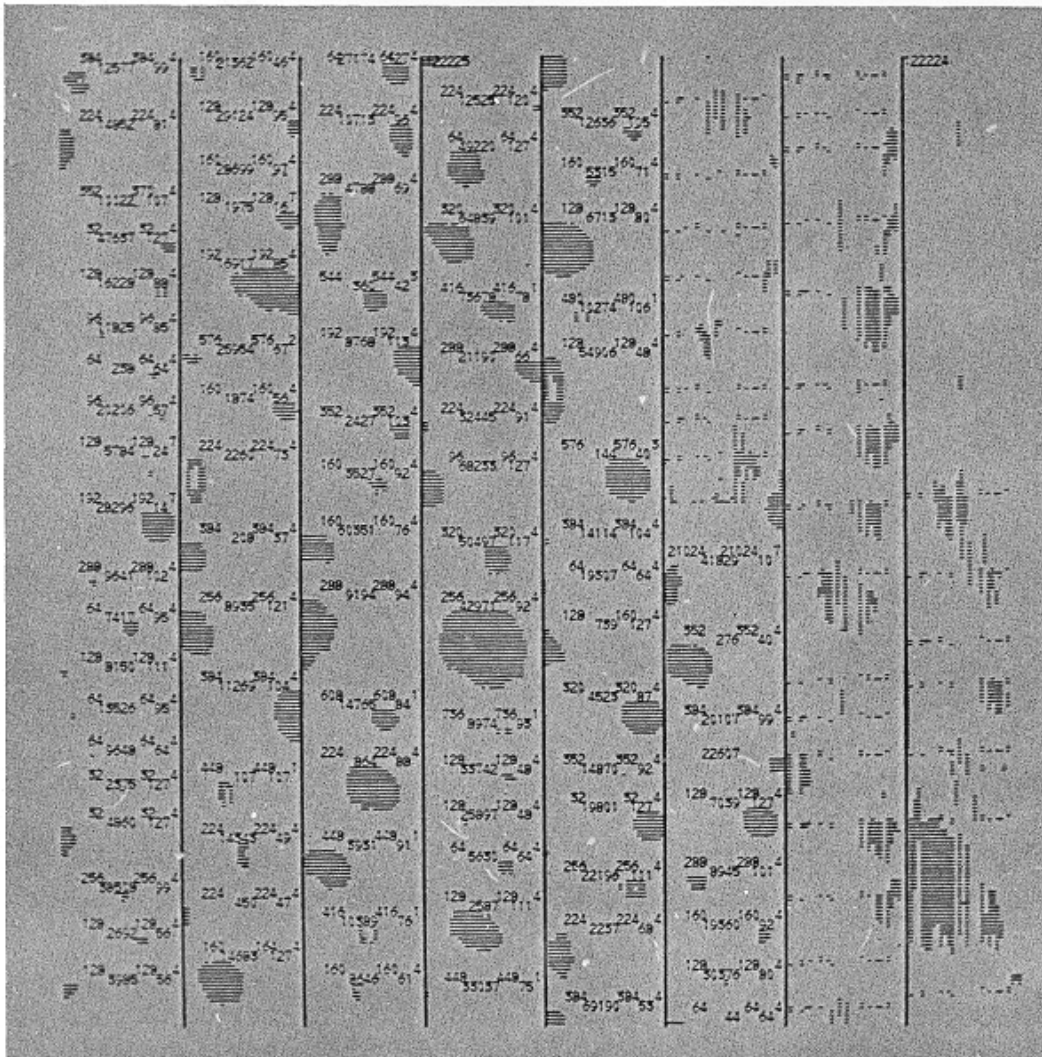


Fig. 23: Sample of PMS 2D probe particle image data from the updraft region of Penetration No. 5 on 10 Aug 1978. Most of the particles appear to be small graupel or columns, probably rimed.



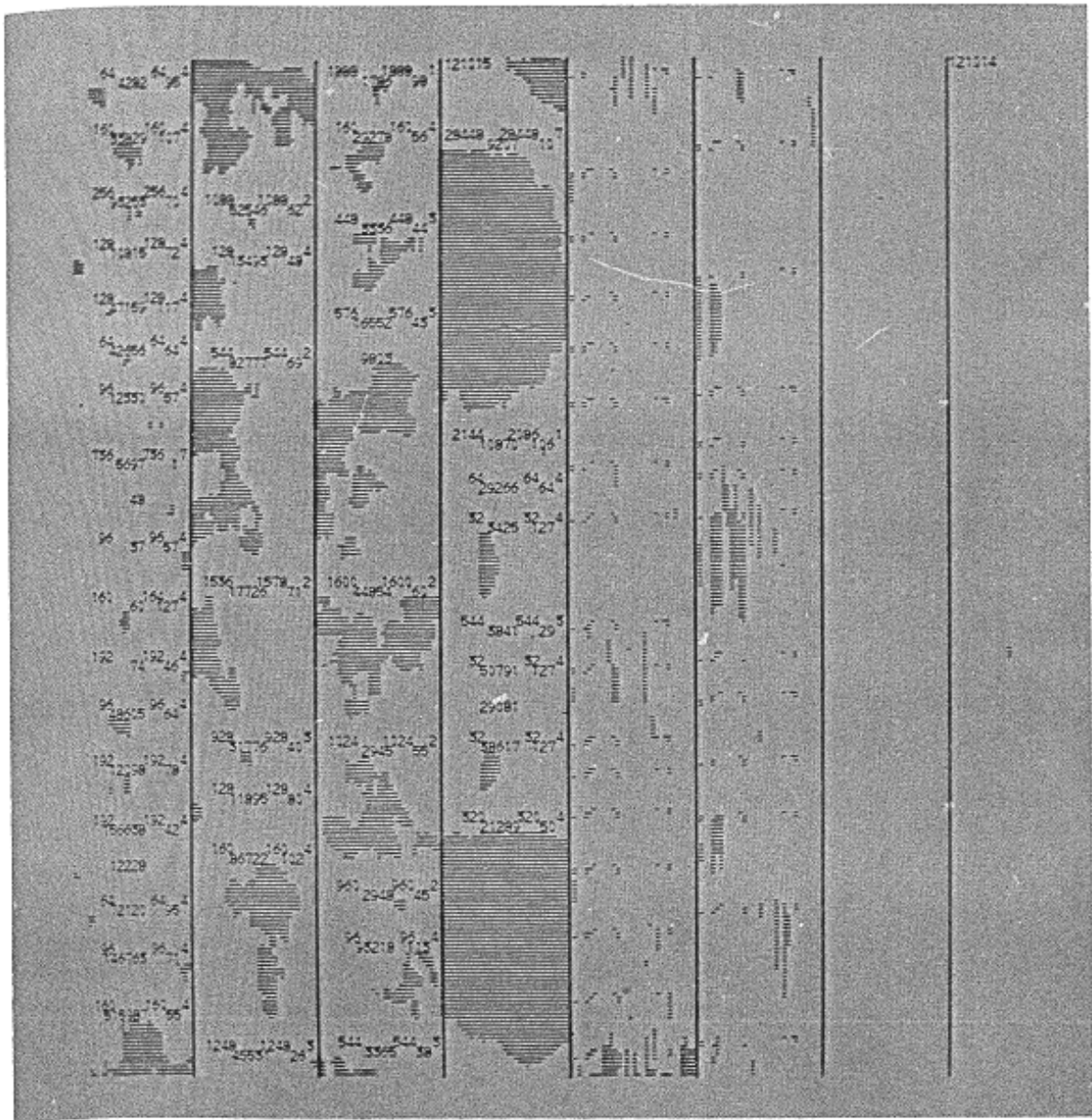


Fig. 24: Example of larger graupel and dendritic or aggregate particles observed by the PMS 2D probe during Penetration No. 2 on 10 Aug 1978.

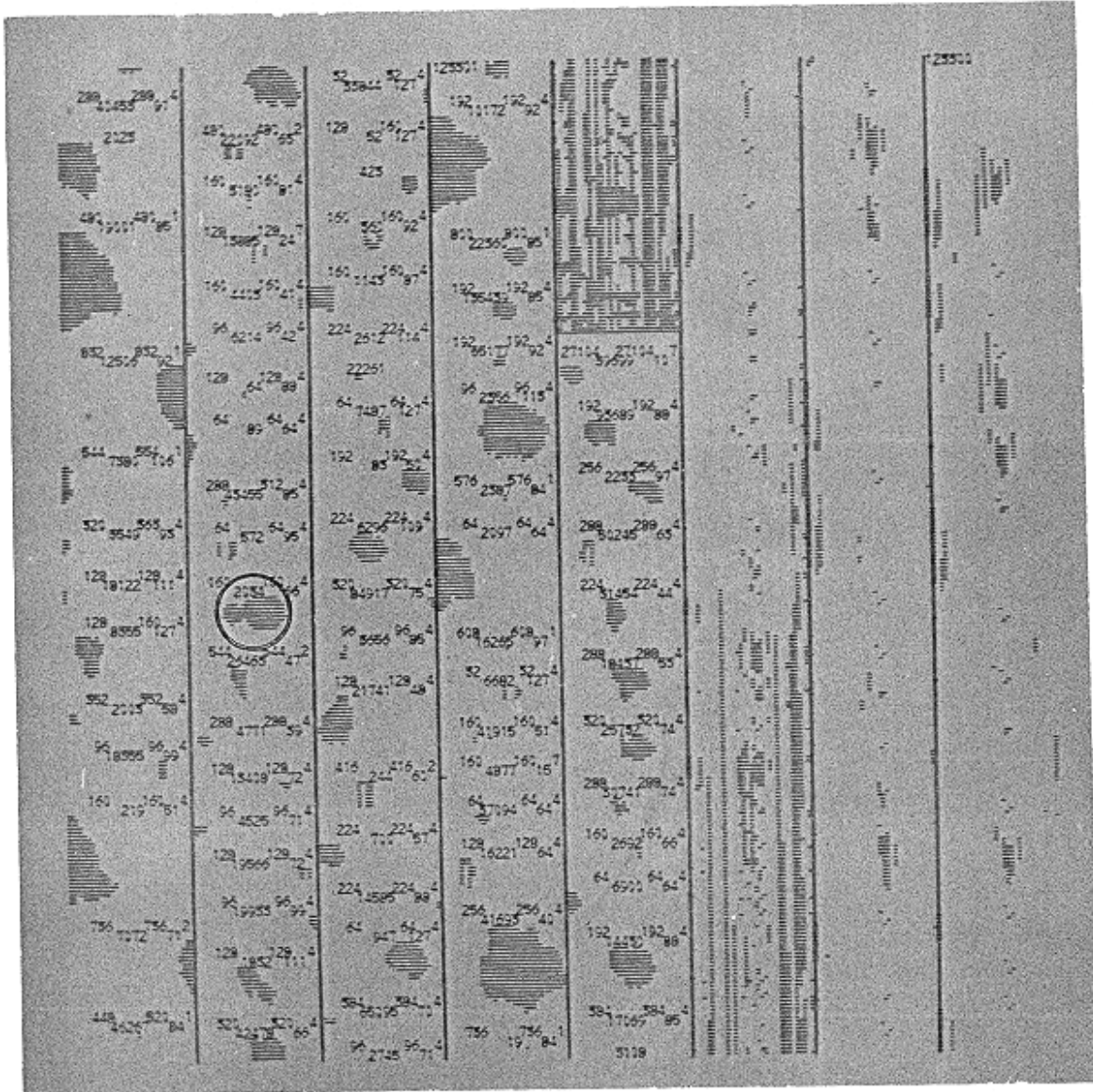


Fig. 25: Sample of PMS 2D probe data from Penetration No. 9 on 10 Aug 1978, showing what appear to be two spherical particles joined together.

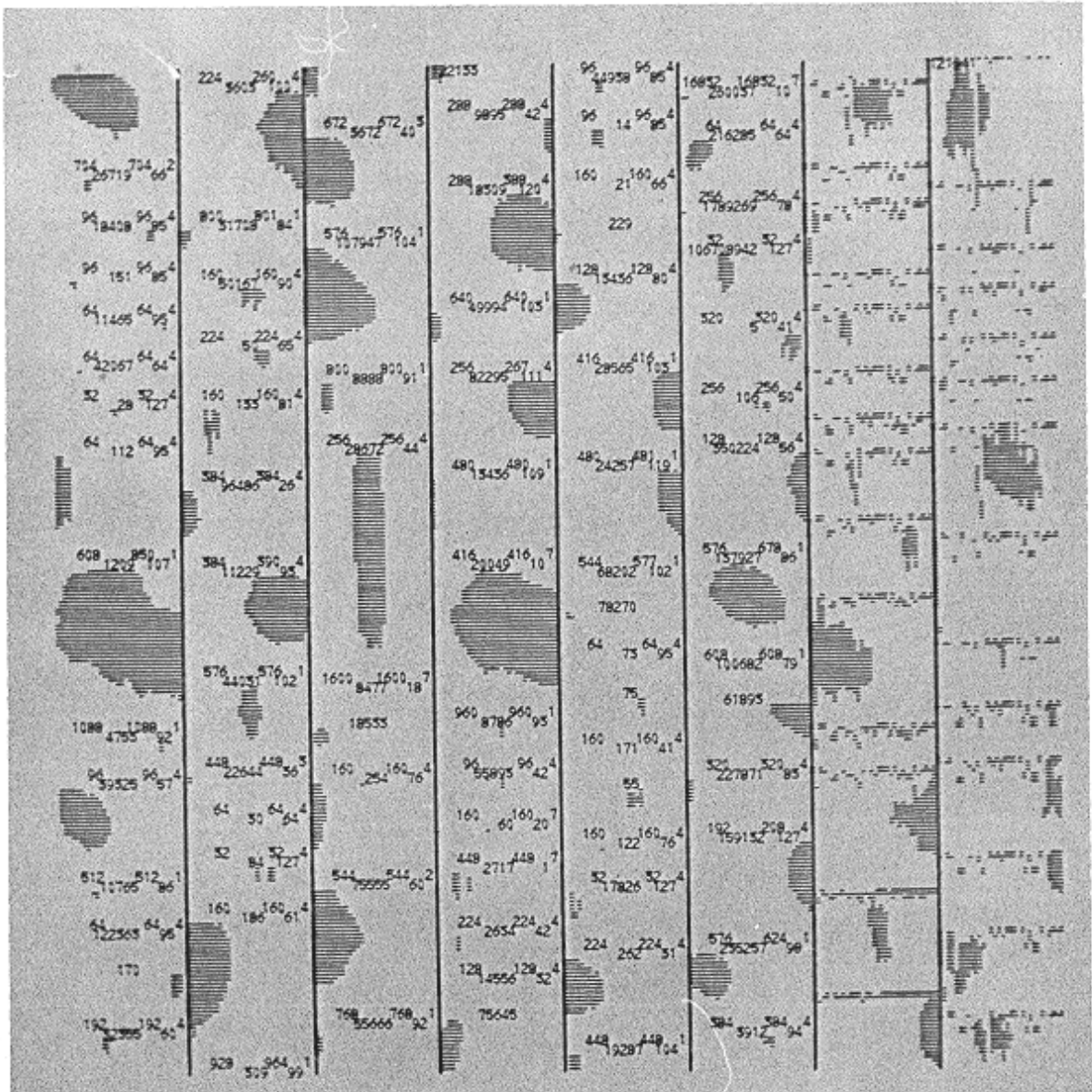


Fig. 26: Sample of PMS 2D probe data from Penetration No. 18 on 12 Aug 1978, showing graupel and columns observed in a weak thunderstorm updraft. -

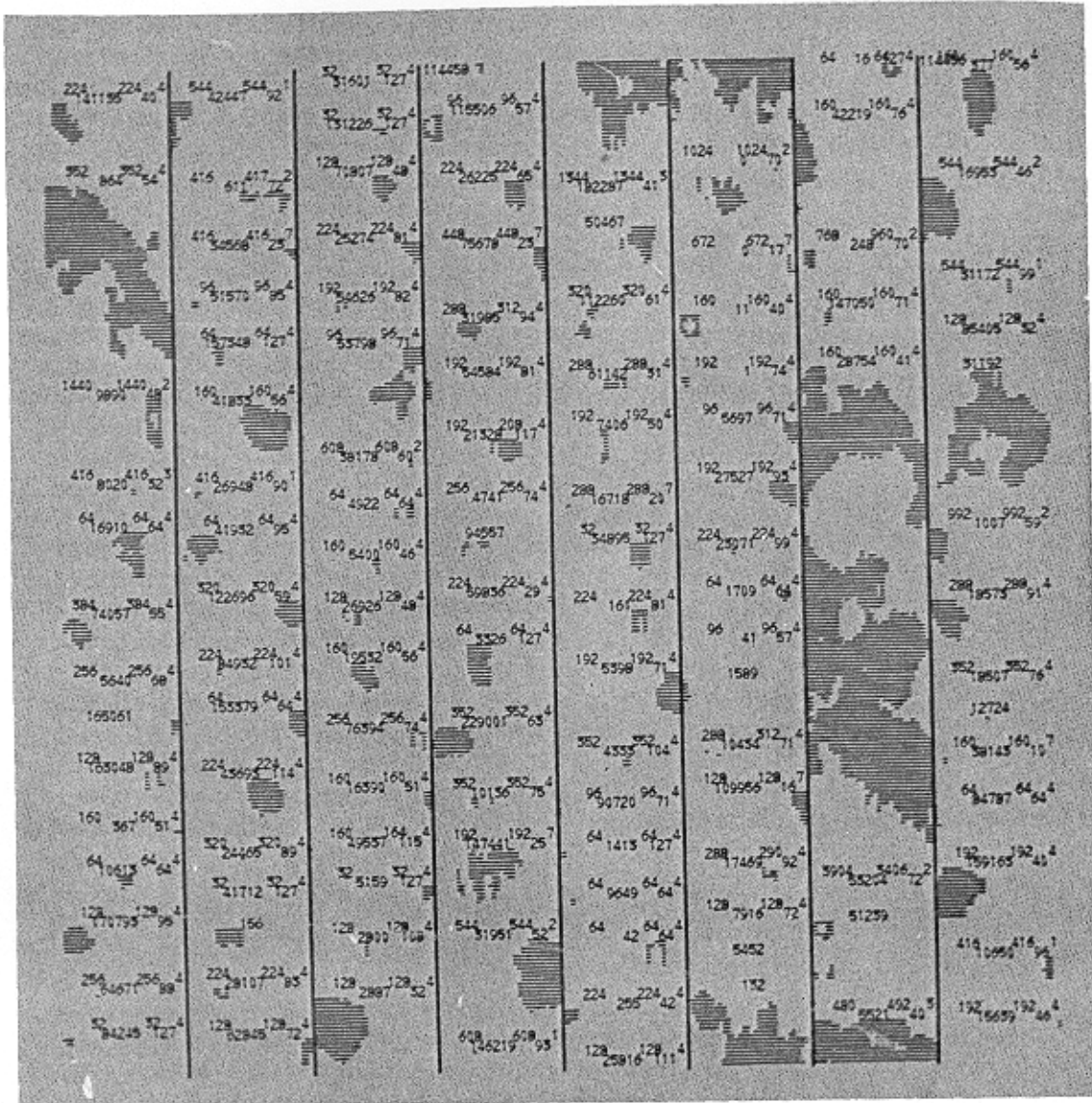


Fig. 27: Example of aggregate-type particles observed by the PMS 2D probe during Penetration No. 5 on 12 Aug 1978.

## 5. SUMMARY AND CONCLUSIONS

The limited set of T-28 observations from TRIP '78 makes it difficult (and somewhat risky) to draw general conclusions about the characteristics of the Florida clouds. Nevertheless, some general features that appeared in the data seem to warrant advancing certain hypotheses about those characteristics. This section first summarizes the observations believed to be most significant and then sets forth some inferences regarding the precipitation and electrification mechanisms.

In evaluating these inferences, the reader should bear in mind another important consideration: the aircraft observations are at best representative of a single line through a storm at a given time. If the line is long, even the simultaneity of the observations along that line cannot be assumed. Such observations provide some estimate of the horizontal structures of the storms but no clue as to their vertical structures. The procedure adopted with the T-28 has been to penetrate each storm repeatedly at essentially a fixed altitude to obtain time history data not convoluted with vertical variations. To see how the storm characteristics vary in the vertical, the penetration altitude is varied among storms. To make inferences about the vertical structure therefore requires comparing observations from different storms, usually on different days. The validity of this procedure depends upon the degree of similarity among the storms considered. With a large sample to choose from, it is possible to find reasonably similar cases, but with the small sample from TRIP '78, the choices are quite limited. While we believe that reasonable comparisons can nevertheless be made, it is clear that more extensive data could lead to modifications, perhaps substantial ones, of some of the ideas presented below.

### 5.1 Summary of Significant Observations

The T-28 penetrations in TRIP '78 were made through the supercooled parts of clouds ranging from small towering cumulus to moderate thunderstorms. None of the storms investigated would be classed as a major electrical storm. All the penetrations were made some 4.5 km or more above cloud base and the measured in-cloud temperatures ranged from about  $-3^{\circ}\text{C}$  to  $-17^{\circ}\text{C}$ . The emphasis in data analysis was placed on the thunderstorm cases. The updrafts and downdrafts were typical for such storms, with the maximum updraft speed somewhat exceeding  $20\text{ m s}^{-1}$ .

The cloud droplet spectra in the TRIP clouds were maritime in character. Droplets up to at least  $45\text{ }\mu\text{m}$  in diameter were always found in the storm updraft regions. The total droplet concentrations were typically of the order of  $200\text{ cm}^{-3}$ . The cloud liquid water concentrations were low in every case, with the maximum J-W value being about  $0.6\text{ g m}^{-3}$ .



High concentrations of "embryo-sized" particles, smaller than 0.5 mm, were found. They were clearly ice particles when the temperature was lower than  $-10^{\circ}\text{C}$ , but the data from regions with higher temperatures were not sufficient to be sure of the particle phases. Most of the particles were roughly circular and appeared to be graupel, but some columnar crystals were also observed.

The precipitation-sized particles, larger than 0.5 mm, were predominantly round as well. Supercooled raindrops were observed, but only in parts of the clouds with temperatures higher than about  $-10^{\circ}\text{C}$ . In some updraft regions warmer than about  $-5^{\circ}\text{C}$ , all the particles were liquid, while between  $-5^{\circ}\text{C}$  and  $-10^{\circ}\text{C}$ , mixtures of liquid and frozen drops were observed. At temperatures below  $-10^{\circ}\text{C}$ , the particles were entirely ice, and appeared to be mainly frozen raindrops. In most cases, the ice particle shapes were somewhat distorted, suggestive of light riming. Several analysts who examined the foil and PMS 2D probe data formed a general impression that the particles tended to be relatively uniform in size. Occasional dendritic or aggregate particles were found, but they occurred in the fringes or the decaying parts of the clouds. The precipitation particle concentrations ranged up to  $10,000\text{ m}^{-3}$ .

The T-28 observations from the Florida clouds are generally consistent with those reported by Hallett *et al.* (1978). The clouds investigated with the T-28 were typically larger than the ones they studied, because the emphasis in TRIP is on thunderstorms. Moreover, the T-28 penetrations were for the most part made later in the cloud life cycles. Thus the updrafts found by the T-28 were generally stronger and the penetrations longer than those discussed by Hallett *et al.* The cloud in their Fig. 5(a) is most similar to the ones discussed in this report.

## 5.2 Inferences Regarding Precipitation Processes

The picture of the precipitation process in the Florida clouds that emerges from the T-28 observations is also similar to that described by Hallett *et al.* (1978). Raindrops observed in updrafts at temperatures only slightly lower than  $0^{\circ}\text{C}$  must have formed by coalescence in the warmer parts of the clouds. The depth of warm cloud and the observed cloud droplet spectra are compatible with an efficient coalescence mechanism. Even in a steady  $15\text{ m s}^{-1}$  updraft, there would be at least 5 minutes available for coalescence to proceed, while the air rose from cloud base to the T-28 penetration altitudes. Moreover, the process evidently converts most of the cloud liquid condensate to embryo- or precipitation-sized particles by the time the air rises above the  $0^{\circ}\text{C}$  level.

The raindrops then freeze in the temperature range from about  $-5^{\circ}\text{C}$  to  $-10^{\circ}\text{C}$ . Mixtures of liquid and frozen drops were found in this range, while at lower temperatures all the precipitation-sized particles were

ice. At a typical net upward speed (updraft minus particle fallspeed) of  $10 \text{ m s}^{-1}$ , the particles would spend only about 1 minute in this region, so the freezing evidently takes place quite rapidly. Hallett et al. remark upon the "rapid proliferation of graupel-sized ice particles."

As in their observations, the T-28 data indicate concentrations of cloud droplets  $25 \mu\text{m}$  in diameter or larger of some tens per cubic centimeter. According to Hallett et al., this is sufficient to produce secondary ice by riming of graupel. Thus once the freezing process begins with a few large drops, a feedback mechanism involving riming of the frozen drops, secondary ice production, capture of the resulting crystals by other raindrops, and subsequent freezing can complete the process rather quickly. Because it seems evident that the coalescence mechanism leads to the initial development of the precipitation particles, the ice phase appears to be incidental rather than essential to the development of precipitation in the TRIP clouds.

The ability of the observed embryo- and precipitation-size particles to consume the cloud liquid water has been established by depletion calculations like those discussed by Musil et al. (1978). The procedure is to first divide the particles into a few broad size categories, usually including particles observed by the PMS 2-D probe, the foil impactor, and the hail spectrometer, respectively. Then the rate of accretion of the observed cloud liquid by particles in each category is computed. A "depletion time" is determined for each category by dividing the observed cloud liquid water concentration by the accretion rate. An example of the results of such calculations for the Florida clouds appears in Fig. 28. The general finding is that in the updraft regions, the observed embryo and precipitation particles are capable of consuming all of the available cloud water in times of the order of 100 seconds.

New condensate, of course, continually adds to the cloud liquid water in the updraft regions. The depletion calculations show that the frozen particles in the updrafts can rapidly consume the cloud liquid water remaining around the  $-5^{\circ}\text{C}$  to  $-15^{\circ}\text{C}$  level. It seems likely that they would also rapidly consume most of any additional cloud liquid condensed during further ascent. The evidence of light riming on the ice particles indicates that such a process takes place. Some aggregate-type particles that did not develop through a coalescence-freezing process were observed, so depositional growth may be important higher up or around the fringes of the updrafts in the clouds.

### 5.3 Inferences Regarding Electrification Processes

The main emphasis of the TRIP investigations is on storm electrical properties and processes. The T-28 observations do not bear directly on these matters, although the updraft data have been used to identify

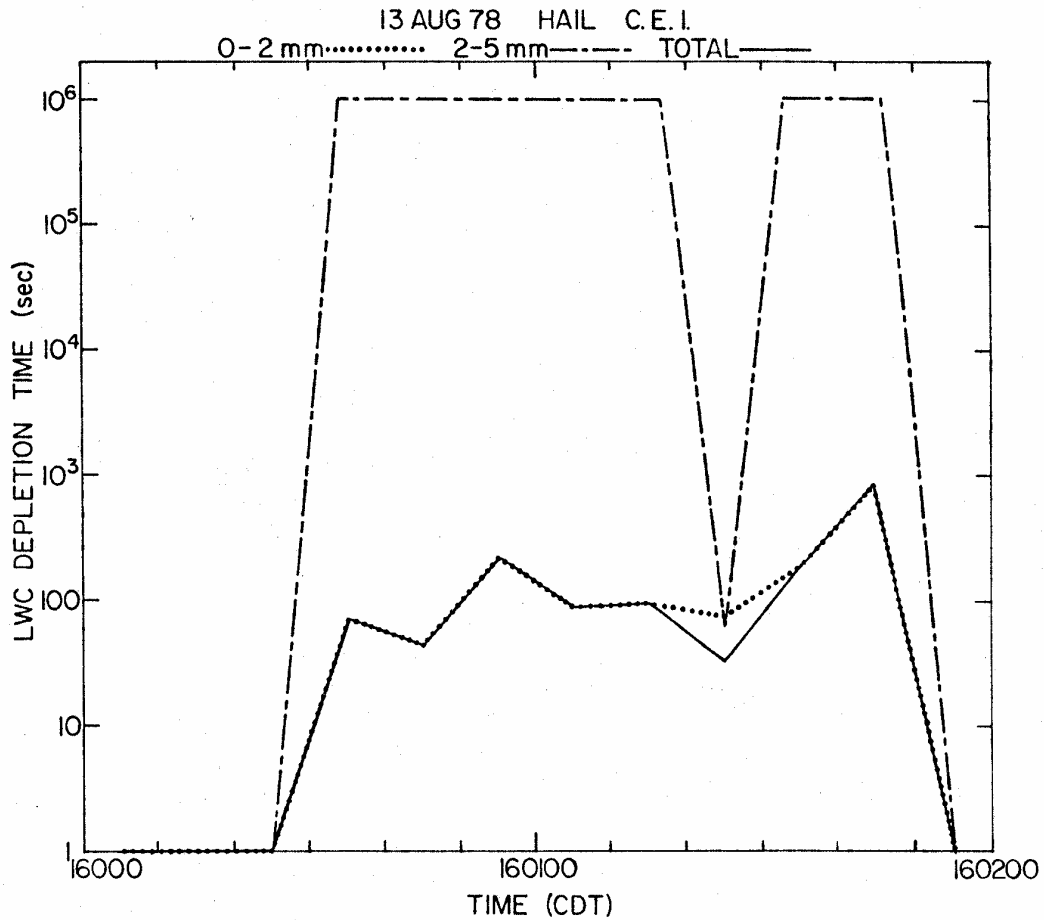


*Fig. 28:* Results of cloud liquid water depletion calculations for a portion of Penetration No. 7 on 13 Aug 1978. Abscissa shows time in minutes, with tick marks at 10-sec intervals corresponding to roughly 1-km segments of the T-28 flight path. Ordinate shows depletion times calculated for particle size categories indicated at top of diagram.



an association between the locations of updraft areas and remotely detected lightning discharge centers (Poehler, 1978). Nevertheless the T-28 microphysics observations provide some evidence useful in determining the electrification processes.

The dominant precipitation initiation process in the TRIP clouds seems to be coalescence. Freezing and subsequent riming of the frozen raindrops occur in the supercooled regions. The observed conditions in the clouds meet the basic requirements for the Hallett-Mossop ice multiplication mechanism which involves riming of graupel with cloud droplets larger than 25  $\mu\text{m}$  in diameter. These factors suggest that hypothetical electrification mechanisms involving ice particles are most likely to be active in the TRIP clouds.

Candidate mechanisms include electrification by splintering during freezing, as suggested by Mason and Maybank (1960) or Kolomeychuk et al. (1975), or the thermoelectric process described by Latham and Mason (1961). Columnar crystals which could have resulted from splintering were sometimes observed by the T-28. On the other hand, this crystal habit could also result from depositional growth in the temperature regime below the flight altitudes. Therefore the origins of the columnar crystals cannot be ascribed with certainty to splintering processes.

Electrification processes associated with the riming of graupel would also be suggested by the T-28 microphysical observations. Thus the mechanism discussed by Aufdermaur and Johnson (1972) may well be active in these clouds. Their experiments showed that some large droplets may collide near the periphery of graupel particles in such a way that part of the water rebounds away. Such events were accompanied by charge separation in the presence of an external electric field.

Charge separation by a similar polarization or induction mechanism involving the rebounding of cloud droplets from raindrops cannot be ruled out by the T-28 observations. Because the coalescence to form raindrops seemed to proceed very efficiently in the TRIP '78 clouds, such a process appears less likely than other possibilities. On the other hand, the theory of this mechanism requires only a small fraction (of the order of 1%) of the droplets to rebound. The aircraft observations are not adequate to rule out such a possibility.

High concentrations of small ice particles were commonly observed by the T-28, so rebounds following collisions between such particles and graupel could occur frequently. However, such interactions are thought to be rather inefficient at separating electrical charge. Thus they probably contribute little to the overall storm electrification.

## ACKNOWLEDGMENTS

The authors are pleased to express their thanks for the contributions of the T-28 field crew: G. N. Johnson, J. E. Leigh, J. Prodan, and J. Weber. We all appreciate the assistance rendered by our hosts at Kennedy Space Center and Patrick Air Force Base, and by numerous other TRIP participants. Dr. A. J. Heymsfield of the NCAR<sup>1</sup> Convective Storms Division supervised the reduction and analysis of the PMS probe data, while Dr. T. W. Cannon analyzed the particle camera film.

Computations related to this research were carried out by J. L. Halvorson at the South Dakota School of Mines and Technology Computation Center and J. L. Parrish at the NCAR<sup>1</sup> Computing Facility.

This research was supported by the Meteorology Program, Division of Atmospheric Sciences, National Science Foundation, under Grant No. ATM78-17326.

---

<sup>1</sup>The National Center for Atmospheric Research (NCAR) is sponsored by the National Science Foundation.

## REFERENCES

- Aufdermaur, A. N., and D. A. Johnson, 1972: Charge separation due to riming in an electric field. Quart. J. Roy. Meteor. Soc., 98, 369-382.
- Gaskell, W., A. J. Illingworth, J. Latham, and C. B. Moore, 1978: Airborne studies of electric fields and the charge and size of precipitation elements in thunderstorms. Quart. J. Roy. Meteor. Soc., 104, 447-460.
- Hallett, J., R. I. Sax, D. Lamb, and A. S. R. Murty, 1978: Aircraft measurements of ice in Florida cumuli. Quart. J. Roy. Meteor. Soc., 104, 631-651.
- Heymsfield, A. J., and J. L. Parrish, 1979: Techniques employed in the processing of particle size spectra and state parameter data obtained with the T-28 aircraft platform. NCAR Technical Note 137+1A, NCAR, Boulder, 78 pp.
- Johnson, G. N., J. H. Killinger, D. J. Musil, and P. L. Smith, Jr., 1978: Cloud physics observations inside hailstorms with an armored aircraft data system. Preprints 4th Symposium on Meteorological Observations and Instrumentation, Denver, Amer. Meteor. Soc., 351-356.
- Knight, C. A., N. C. Knight, W. W. Grotewold, and T. W. Cannon, 1977: Interpretation of foil impactor impressions of water and ice particles. J. Appl. Meteor., 16, 997-1002.
- Kolomeychuk, R. J., D. C. McKay, and J. V. Iribarne, 1975: The fragmentation and electrification of freezing drops. J. Atmos. Sci., 32, 974-979.
- Latham, J., and B. J. Mason, 1961: Generation of electric charge associated with the formation of soft hail in thunderclouds. Proc. Roy. Soc., A260, 537-549.
- Lhermitte, R., 1978: Doppler radar and electrical radiation observations of thunderstorms. Preprints Conf. Cloud Physics and Atmos. Elec., Issaquah, WA, Amer. Meteor. Soc., 582-587.
- Livingston, J. M., and E. P. Krider, 1978: Electric fields produced by Florida thunderstorms. J. Geophys. Res., 83, 385-401.
- Mason, B. J., and J. Maybank, 1960: The fragmentation and electrification of freezing water drops. Quart. J. Roy. Meteor. Soc., 86, 176-186.

- Musil, D. J., P. L. Smith, Jr., and A. J. Heymsfield, 1978: Total hydrometeor spectra in a hailstorm and implications for precipitation growth processes. Preprints Conf. Cloud Physics and Atmos. Elec., Issaquah, WA, Amer. Meteor. Soc., 173-177.
- Pierce, E. T., 1976: The Thunderstorm Research International Program (TRIP) - 1976. Bull. Amer. Meteor. Soc., 57, 1214-1216.
- Poehler, H. A., 1978: A preliminary test of the application of the lightning detection and ranging system (LDAR) as a thunderstorm warning and location device for the FAA including a correlation with updrafts, turbulence, and radar precipitation echoes. NASA Contractor Report CR-154629, National Aeronautics and Space Administration, John F. Kennedy Space Center. 29 pp.
- Sand, W. R., J. L. Halvorson, and T. G. Kyle, 1976: Turbulence measurements inside thunderstorms used to determine diffusion characteristics for cloud seeding. Preprints 2nd WMO Scientific Conf. Wea. Modif., WMO No. 443, 539-545.
- Spyers-Duran, P. A., 1968: Comparative measurements of cloud liquid water using heated wire and cloud replicating devices. J. Appl. Meteor., 7, 674-678.